

1  
2 Functions of *Gtf2i* and *Gtf2ird1* in the developing brain: transcription, DNA-binding,  
3 and long term behavioral consequences.

4  
5  
6 **Authors:**

7 Nathan D. Kopp<sup>1,2</sup>, Kayla R. Nygaard<sup>1,2</sup>, Katherine B. McCullough<sup>1,2</sup>, Susan E. Maloney<sup>2,3</sup>,  
8 Harrison W. Gabel<sup>4</sup>, Joseph D. Dougherty<sup>1,2,3,\*</sup>

9  
10  
11 **Affiliations:**

12  
13 <sup>1</sup>Department of Genetics, Washington University School of Medicine, St. Louis, MO, USA

14 <sup>2</sup>Department of Psychiatry, Washington University School of Medicine, St. Louis, MO, USA

15 <sup>3</sup>Intellectual and Developmental Disabilities Research Center, Washington University School  
16 of Medicine, St. Louis, MO, USA

17 <sup>4</sup>Department of Neuroscience, Washington University School of Medicine, St Louis MO, USA  
18

19 **Contact Information:**

20 Dr. Joseph Dougherty

21 Department of Genetics

22 Campus Box 8232

23 4566 Scott Ave.

24 St. Louis, MO. 63110-1093

25 P: 314-286-0752

26 F: 314-362-7855

27 E: [jdougherty@wustl.edu](mailto:jdougherty@wustl.edu)  
28  
29  
30  
31  
32  
33  
34  
35  
36  
37  
38  
39  
40  
41  
42  
43  
44  
45  
46  
47  
48

1  
2  
3  
4  
5  
6  
7  
8  
9  
10  
11  
12  
13  
14  
15  
16  
17  
18  
19  
20  
21  
22  
23  
24  
25

**Abstract**

*Gtf2ird1* and *Gtf2i* may mediate aspects of the cognitive and behavioral phenotypes of Williams Syndrome (WS) – a microdeletion syndrome encompassing these transcription factors (TFs). Knockout mouse models of each TF show behavioral phenotypes. Here we identify their genomic binding sites in the developing brain, and test for additive effects of their mutation on transcription and behavior. Both TFs target constrained chromatin modifier and synaptic protein genes, including a significant number of ASD genes. They bind promoters, strongly overlap CTCF binding and TAD boundaries, and moderately overlap each other, suggesting epistatic effects. We used single and double mutants to test whether mutating both TFs will modify transcriptional and behavioral phenotypes of single *Gtf2ird1* mutants. Despite little difference in DNA-binding and transcriptome-wide expression, *Gtf2ird1* mutation caused balance, marble burying, and conditioned fear phenotypes. However, mutating *Gtf2i* in addition to *Gtf2ird1* did not further modify transcriptomic or most behavioral phenotypes, suggesting *Gtf2ird1* mutation alone is sufficient.

1

## 2 **Introduction**

3

4       The Williams syndrome critical region (WSCR) contains 28 genes that are  
5 typically deleted in Williams syndrome (WS) (OMIM#194050). The genes in this  
6 region are of interest for their potential to contribute to the unique physical,  
7 cognitive, and behavioral phenotypes of WS, which include craniofacial  
8 dysmorphism, mild to severe intellectual disability, poor visuospatial cognition,  
9 balance and coordination problems, and a characteristic hypersocial personality (1–  
10 3). Single gene knockout mouse models exist for many of the genes in the region,  
11 with differing degrees of face validity for WS phenotypes (4–9). Two genes have  
12 been highlighted in the human and mouse literature as playing a large role in the  
13 social and cognitive tasks: *Gtf2i* and *Gtf2ird1*. Mouse models of each gene have  
14 shown social phenotypes as well as balance and anxiety phenotypes (4,8–12). Since  
15 evidence shows that each gene affects similar behaviors, we set out to test the  
16 hypothesis that simultaneous knockdown of both genes would cause more severe  
17 phenotypes. Investigating the genes together, rather than individually, could  
18 provide a more complete understanding of how the genes in the WSCR contribute to  
19 the phenotypes of WS.

20       *Gtf2i* and *Gtf2ird1* are part of the General Transcription Factor 2i family of  
21 genes. A third member, *Gtf2ird2*, is located in the WSCR that is variably deleted in  
22 WS patients with larger deletions (13). This gene family arose from gene duplication  
23 events, resulting in high sequence homology between the genes (14). The defining

1 feature of this gene family is the presence of the helix-loop-helix I repeats, which are  
2 involved in DNA and protein binding (15). *Gtf2i*'s roles include regulating  
3 transcriptional activity in the nucleus. However, this multifunctional transcription  
4 factor also exists in the cytoplasm where it conveys messages from extracellular  
5 stimuli and regulates calcium entry into the cell (16,17). So far, *Gtf2ird1* has only  
6 been described in the nucleus of cells and is thought to regulate transcription and  
7 associate with chromatin modifiers (18). The DNA binding of these two  
8 transcription factors (TFs) has only been studied in ES cells and embryonic  
9 craniofacial tissue. They recognize similar and disparate genomic loci, suggesting  
10 the proteins interact to regulate specific regions of the genome (19,20). However,  
11 binding of these TFs has not been studied in the developing brain, which could  
12 provide more relevant insight on how the General Transcription Factor 2i family  
13 contributes to cognitive and behavioral phenotypes.

14 We performed ChIP-seq on GTF2I and GTF2IRD1 in the developing mouse  
15 brain to define where these TFs bind and then tested the downstream consequences  
16 of disrupting this binding. We used the CRISPR/Cas9 system to make a mouse model  
17 with a mutation in *Gtf2ird1* alone and a mouse model with mutations in both *Gtf2i*  
18 and *Gtf2ird1* to test how adding a *Gtf2i* mutation modifies the effects of *Gtf2ird1*  
19 mutation. We showed the mutation in *Gtf2ird1* resulted in the production of an N-  
20 truncated protein that disrupts the binding of GTF2IRD1 at the *Gtf2ird1* promoter  
21 and deregulates the transcription of *Gtf2ird1*, moderately decreasing protein levels  
22 so homozygous mutants approximate levels expected from hemizyosity of the  
23 WSCR. While there are mild consequences of the mutation on genome-wide

1 transcription, the mutant mouse exhibited clear balance, marble burying, and  
2 conditioned fear differences. Comparing the single gene mutant to the double  
3 mutant did not reveal more severe transcriptional changes and behavioral  
4 phenotypes, however adding *Gtf2i* on top of a background of two *Gtf2ird1* mutations  
5 resulted in abnormal pre-pulse inhibition and cued fear conditioning. This suggests  
6 *Gtf2ird1* drives the majority of the phenotypes observed in current studies, and total  
7 protein level, N-terminal truncation, or both have functional consequences on DNA-  
8 binding and behavior.

9

## 10 **Results**

11

12 *Gtf2i and Gtf2ird1 bind at active promoters and conserved sites*

13

14 The paralogous transcription factors, GTF2I and GTF2IRD1, have been  
15 implicated in the behavioral phenotypes seen in humans with WS as well as mouse  
16 models (4,8,11,12,21,22). However, the underlying mechanisms by which the  
17 General Transcription Factor 2i family acts are not well understood. One approach  
18 to begin to identify how these TFs can regulate phenotypes is by identifying where  
19 they bind in the genome. This has been done in ES cells and embryonic facial tissue  
20 and revealed that both of these transcription factors bind to genes involved in  
21 craniofacial development (19). However, these are not relevant tissues when  
22 considering phenotypes related to brain development and subsequent behavior. To  
23 address this, we performed ChIP-seq for GTF2IRD1 and GTF2I in the developing

1 brain at embryonic day 13.5 (E13.5), a time point when both of these proteins are  
2 highly expressed (23).

3 We identified 1,410 peaks that were enriched in the GTF2IRD1 IP samples  
4 compared to the input (**Supplemental Table 1**). The GTF2IRD1-bound regions  
5 were strikingly enriched in the promoters of genes and along the gene body, more  
6 so than would be expected by randomly sampling the genome (**Figure 1A**) ( $\chi^2 =$   
7 1537.8, d.f. =7,  $p < 2.2 \times 10^{-16}$ ). The bound peaks were found mostly in H3K4me3  
8 bound regions (OR=779.5,  $p < 2.2 \times 10^{-16}$  Fisher's exact test (FET)), suggesting they are  
9 in active sites in the genome. While GTF2IRD1-bound regions were also enriched in  
10 repressed regions of the genome as defined by H3K27me3 marks (OR=4.090,  $p <$   
11  $2.2 \times 10^{-16}$  FET), only 11% of GTF2IRD1 peaks were found in H3K27me3 regions as  
12 opposed to 94% in H3K4me3 regions (**Figure 1B**), suggesting GTF2IRD1 may have  
13 more of a role in activation than repression.

14 To understand the common functions of the genes that have GTF2IRD1  
15 bound at the promoter we performed a GO analysis. The top ten results were  
16 consistent with the functions previously described for GTF2IRD1, specifically  
17 regulation of transcription and chromatin organization, but also identified new  
18 categories, such as protein ubiquitination (**Figure 1C**). To further test these regions  
19 for functional consequences, we compared the conservation of GTF2IRD1-bound  
20 peaks to a random sample of the genome and found the GTF2IRD1 peaks are more  
21 conserved ( $t=18.131$ , d.f.=2403,  $p < 2 \times 10^{-16}$ ) (**Figure 1D**). We conducted motif  
22 enrichment analysis using HOMER to identify other factors that share binding sites  
23 with GTF2IRD1 (**Figure 1E**). The GSC motif, which is similar to the core RGATTR

1 motif for GTF2I and GTF2IRD1, was identified in 4.64% of the targets (24).  
2 Interestingly, the CTCF motif was found at 11% of the GTF2IRD1 targets. These  
3 findings suggest the GTF2i may modulate chromatin organization both through its  
4 direct binding at CTCF sites and through regulation of chromatin modifier genes.

5 GTF2I ChIP-seq showed similar results to those of GTF2IRD1. We identified  
6 1,755 (**Supplemental Table 2**) WT GTF2I peaks that had significantly higher  
7 coverage in the WT IP compared to the KO IP (**Supplemental Figure 1A**). These  
8 peaks were significantly enriched for promoter regions as well as the gene body  
9 when compared to random genomic targets (**Figure 2A**)( $\chi^2 = 911.63$ , d.f.=7,  $p <$   
10  $2.2 \times 10^{-16}$ ). Like GTF2IRD1, the majority of the GTF2I peaks (78.7%) overlapped  
11 H3K4me3 peaks (OR=160.98,  $p < 2.2 \times 10^{-16}$  FET), with a smaller subset of peaks  
12 (20.7%) overlapping with the H3K27me3 mark (OR 7.022,  $p < 2.2 \times 10^{-16}$  FET). This  
13 suggests that these peaks are located mainly in active regions of the genome (**Figure**  
14 **2B**). Summarizing the common functions of these target genes by GO analysis  
15 showed enrichment for biological processes such as intracellular signal  
16 transduction and phosphorylation (**Figure 2C**). For example, GTF2I binds within the  
17 gene body of the *Src* gene (**Figure 2D**), which has been shown to phosphorylate  
18 GTF2I in order to activate its transcriptional activity as well as regulate calcium  
19 entry into the cell (16,17). The GTF2I binding sites are also significantly more  
20 conserved than random sampling of the genome, further suggesting important  
21 functional roles of these regions (**Figure 2E**). Motif enrichment of the GTF2I peaks  
22 revealed GC rich binding motifs, such as for the KLF and SP families of transcription  
23 factors, as well as Lhx family members. Finally, we see an enrichment of the CTCF

1 motif, which is fitting as GTF2I has been shown to help target CTCF to specific  
2 genomic regions (25) (**Figure 2F**).

3

4 *Gtf2i* and *Gtf2ird1* binding sites have distinct features, yet overlap at a subset of  
5 promoters

6

7 One way in which GTF2I and GTF2IRD1 can interact is by binding the same  
8 sites in the genome. We therefore directly compared the regions bound by these  
9 proteins. First, we compared the GTF2I and GTF2IRD1 ChIP peaks and found the  
10 pattern of their binding sites is significantly different ( $\chi^2 = 282.84$ , d.f.=7,  $p < 2.2 \times 10^{-16}$ ) (**Figure 3A**); while both transcription factors mainly bind in promoters and the  
11 gene body, GTF2IRD1 has a higher proportion of peaks at the promoter compared to  
12 GTF2I, whereas GTF2I has more peaks at intergenic regions. Interestingly, when we  
13 compared them directly to each other, the GTF2IRD1-bound peaks were  
14 significantly more conserved than the GTF2I-bound peaks ( $t=7.81$ , d.f.=2736.5,  
15  $p=8.2 \times 10^{-15}$ ) (**Figure 3B**). Next, to identify common targets, we identified the genes  
16 with both transcription factors at their promoter and found a significant overlap of  
17 148 genes ( $p < 1 \times 10^{-38}$  FET) (**Figure 3C**). Motif analysis on the shared peaks showed  
18 further enrichment of both CTCF and GSC motifs (**Figure 3D**).

19

20  
21 The GO functions of the overlapped genes highlight specific roles in synaptic  
22 functioning and signal transduction (**Figure 3E**). *Mapk14* is an example of a gene  
23 involved in signal transduction that has both GTF2I and GTF2IRD1 bound at its



1 promoter (**Figure 3F**). Shared targets such as this suggest that there are points of  
2 convergence where deleting both genes, such as in WS, might result in synergistic  
3 downstream impacts.

4 Finally, given the consistent enrichment of CTCF binding sites in both GTF2I  
5 and GTF2IRD1 bound regions, we also compared the targets for each transcription  
6 factor to CTCF targets in E14.5 whole brain (26). We found a highly significant  
7 overlap between GTF2IRD1 and CTCF peaks, with roughly two-thirds of GTF2IRD1  
8 binding overlapping with CTCF bound sites (939 shared peaks, OR=89.60,  $p <$   
9  $2.2 \times 10^{-16}$  FET). Similarly, GTF2I shared more peaks in common with CTCF (43%)  
10 than we would expect by chance (756 shared peaks, OR=28.16,  $p <$   $2.2 \times 10^{-16}$  FET).  
11 Next, since CTCF has been shown to be present at topological associating domain  
12 (TAD) boundaries, we compared the GTF2IRD1 and GTF2I peaks with TAD  
13 boundaries determined in E14.5 cortical neurons and found significant overlaps  
14 (557 shared peaks, OR =0.16,  $p <$   $2.2 \times 10^{-16}$  FET and 451 shared peaks, OR=5.19,  $p <$   
15  $2.2 \times 10^{-16}$  FET, respectively).

16 Thus, this TF family is remarkably enriched at promoters of neural genes,  
17 overlaps substantially at regions binding the chromatin looping protein CTCF, and is  
18 highly enriched a subset of TAD boundaries detected in the developing mouse brain.  
19 Overall, these TFs are poised to be important regulators of neural development and  
20 thus might regulate other genes associated with developmental diseases.

21

22 *Gtf2i and Gtf2ird1 bind promoters of known autism genes.*

23

1 Copy number variations in the WS locus are clearly associated with autism  
2 spectrum disorder (27) and recent exome and genome sequencing analyses have  
3 identified over 100 more associated loci, mostly containing single genes where loss  
4 of function mutations can cause ASD (28). Interestingly, these genes are  
5 substantially enriched in chromatin modifiers and transcriptional regulators, just  
6 like GTF2IRD1 targets. However, it is unclear how mutations in this wide variety of  
7 genes all lead to a common cognitive phenotype. One widely proposed possibility is  
8 these genes are part of a functional network and mutation of any one gene might  
9 disrupt some core facet of transcriptional regulation, though most of the evidence to  
10 support this idea comes from analyses of co-expression across development (29),  
11 rather than any measure of functional interaction or targeted regulation. Therefore,  
12 we next examined whether GTF2IRD1 and GTF2I are positioned to regulate other  
13 ASD genes by binding within them or nearby. We found that GTF2IRD1 targets were  
14 highly enriched for ASD genes (OR >3.5, p-value <1.5x10<sup>-5</sup> FET) – targeting 19 of the  
15 102 genes, including a variety of epigenetic regulators such as DNMT3A, SETD5,  
16 NSD1, ADNP and SIN3A (**Figure 3G**). GTF2IRD1 was generally bound to their  
17 promoters or nearby CpG islands, suggesting direct regulation of these genes. GTF2I  
18 was likewise enriched at ASD genes, albeit more moderately (OR=2.1, p<.02 FET),  
19 targeting 14 genes. Five genes were targeted by both (**Figure 3G**). Thus our DNA  
20 binding data supports prior coexpression data that suggests a subset of ASD genes  
21 may be part of an interrelated module of chromatin modifying genes, and is  
22 consistent with prior suggestions that this convergence indicates these genes may  
23 have similar downstream pathways leading to disease (30).

1           It has also been found that genes mutated in ASD tend to be highly  
2 constrained in the general human population, with almost no loss of function  
3 mutations observed across >140,000 exome sequencing samples (summarized as a  
4 pLI score of >.9)(31). Strong constraint, even of heterozygous loss of function  
5 mutations, suggests that these genes do not tolerate decreased expression and thus  
6 require a very precise amount of transcription for normal human survival or  
7 reproductive fitness. We find >30% of GTF2IRD1-bound genes meet this criterion, a  
8 result highly unlikely to be due to chance (OR=2.48, p-value<2.2x10<sup>-16</sup> FET). GTF2I  
9 targets also show a significant, but more modest, enrichment (OR=1.27, p-  
10 value<1.1x10<sup>-7</sup> FET) (**Figure 3G**). Together, these results show that these TFs,  
11 especially GTF2IRD1, tend to bind genes requiring tight regulation of expression, as  
12 indicated by severe phenotypes and intolerance to loss of function mutations.

13

14   *Frameshift mutation in Gtf2ird1 results in truncated protein and affects DNA binding*  
15   *at the Gtf2ird1 promoter*

16

17           To investigate the functional role of *Gtf2ird1* and *Gtf2i* at these bound sites  
18 and understand how these genes interact, we made loss of function models of  
19 *Gtf2ird1* individually and a double mutant with mutations in both *Gtf2i* and *Gtf2ird1*.  
20 We designed one gRNA for each gene and injected them simultaneously into FVB/NJ  
21 mouse embryos to obtain single and double gene mutations. We first characterized  
22 the consequences of a one base pair adenine insertion in exon three of *Gtf2ird1*. This  
23 frameshift mutation introduces a premature stop codon in exon three, an early

1 constitutively expressed exon, which we expected to trigger nonsense-mediated  
2 decay (**Figure 4A**). We crossed heterozygous mutant animals to analyze *Gtf2i* and  
3 *Gtf2ird1* transcript and protein abundance in heterozygous and homozygous  
4 mutants compared to WT littermates (**Figure 4B**). The western blots and qPCR  
5 were performed using the whole brain at E13.5. As expected, the *Gtf2ird1* mutation  
6 did not affect *Gtf2i* transcript or protein levels (**Figure 4C,D**). Contrary to our  
7 prediction of nonsense-mediated decay, we observed a 1.74-fold increase in the  
8 *Gtf2ird1* transcript with each copy of the mutation and a 40% reduction of the  
9 protein in homozygous mutants compared to WT with no significant difference  
10 between the WT and heterozygous mutants (**Figure 4E, F**). This suggests the  
11 mutation did have an effect on protein abundance and disrupted the normal  
12 transcriptional regulation of the gene, with the homozygous mutant modeling  
13 protein levels that might be expected in WS.

14 We noticed a slight shift in the homozygous mutant band, which may  
15 correspond to loss of the N-terminal end of the protein. Similar results were  
16 reported in another mouse model that deleted exon two of *Gtf2ird1*, in which lower  
17 levels of an N-terminally truncated protein was caused by a translation re-initiation  
18 event at methionine-65 in exon three (32). The N-terminal end codes for a  
19 conserved leucine zipper, which participates in dimerization as well as DNA-binding  
20 (32,33). Mutating the leucine zipper was shown to affect binding of the protein to  
21 the *Gtf2ird1* upstream regulatory (GUR) element located at the promoter of *Gtf2ird1*.  
22 Given the previous findings that GTF2IRD1 negatively autoregulates its own  
23 transcription and mutating the leucine zipper affects binding to the GUR, we

1 hypothesized that the frameshift mutation diminished the ability of GTF2IRD1 to  
2 bind its promoter resulting in increased transcript abundance. We tested this by  
3 performing ChIP-qPCR in the E13.5 brain in WT and *Gtf2ird1*<sup>-/-</sup> mutants. In the WT  
4 brain, GTF2IRD1 IP enriched for the GUR 13-20 times over off-target sequences,  
5 which was significantly higher than the GTF2IRD1 IP in the *Gtf2ird1*<sup>-/-</sup> brain (**Figure**  
6 **4G,H,I**). Taken together, nonsense transcripts of *Gtf2ird1* with a stop codon in exon  
7 3 can reinitiate at a lower level to produce a N-truncated protein with diminished  
8 binding capacity at the GUR element.

9

#### 10 *Truncated GTF2IRD1 does not affect binding genome wide*

11         Given that the one base pair insertion did not result in a full knockout of the  
12 protein but did affect its DNA binding capacity at the GUR of *Gtf2ird1*, we tested  
13 whether the mutant was a loss of function for all DNA binding. We performed ChIP-  
14 seq in the E13.5 *Gtf2ird1*<sup>-/-</sup> mutants and compared it to WT ChIP-seq data. This  
15 comparison confirmed the decrease in binding at the TSS of *Gtf2ird1*, suggesting the  
16 mutation has greatly decreased binding at this locus (**Figure 4J**). Surprisingly, the  
17 only peak identified as having differential coverage (FDR < 0.1) between the two  
18 genotypes was the peak at the *Gtf2ird1* TSS (**Figure 4K**). This suggests that the  
19 frameshift mutation has a very specific consequence on how GTF2IRD1 binds to its  
20 own promoter that does not robustly affect its binding elsewhere in the genome.  
21 The *Gtf2ird1* promoter has two instances of the R4 core motif in the sense direction  
22 and one instance of the motif in the antisense orientation. We searched the  
23 sequences under the identified peaks for similar orientations of this binding motif

1 and found three other peaks, none of which showed any difference in binding  
2 coverage between genotypes. However, these three other peaks did not match the  
3 exact spacing of the R4 motifs found in the *Gtf2ird1* promoter. This suggests that the  
4 leucine zipper is important for a specific configuration of binding sites that is only  
5 present in this one instance in the genome. It has been shown that the three R4  
6 motifs are present in the same orientation and spacing across great evolutionary  
7 distances (32).

8

9 *Gtf2ird1* frameshift mutation shows mild transcriptional differences

10

11 The N-truncation of GTF2IRD1 clearly affected its binding at the *Gtf2ird1*  
12 promoter and affected expression levels. Although we didn't see genome-wide  
13 binding perturbed, it is possible losing the N terminus, or the decreased protein  
14 level, altered the protein's ability to recruit other transcriptional co-regulators to  
15 impact gene expression. Therefore, we tested the effects of this mutation on  
16 genome-wide transcription in the E13.5 brain. We compared the whole brain  
17 transcriptome of WT littermates to heterozygous and homozygous mutants.  
18 Strikingly similar to ChIP-seq data, the only transcript with an FDR < 0.1 was  
19 *Gtf2ird1*, which was affected in the same direction seen in the qPCR results (**Figure**  
20 **4L** and **Supplemental Figure 2A**). We leveraged WT ChIP-seq data to test if  
21 GTF2IRD1 presence at a promoter correlates with gene expression. Binning the  
22 genes according to expression level showed that the distribution of GTF2IRD1  
23 targets was different than expected by chance ( $\chi^2 = 48.83$ , d.f.=3  $p < 1.42 \times 10^{-10}$ ),

1 suggesting highly expressed genes are more likely to have GTF2IRD1 bound at their  
2 promoters (**Figure 4M**). The majority (1262 peaks) of the GTF2IRD1 peaks at a TSS  
3 were at expressed genes, with only 410 next to genes not expressed at detectable  
4 levels in the E13.5 brain. To see if there was a more subtle general effect below our  
5 sensitivity to detect by analysis of single genes, we tested the bound GTF2IRD1  
6 targets expressed as a population for a shift in expression. We saw a trend towards  
7 significance between the bound and unbound genes, but with a small effect size: a  
8 mean increase of 0.014 fold change in GTF2IRD1 targets (Kolmogorov-Smirnov  
9 test  $D=0.038$ ,  $p=0.079$ ). While this is perhaps unsurprising because the frameshift  
10 mutation did not disturb binding genome wide (**Figure 4N**), the homozygous  
11 mutants do have an overall decrease in protein level of ~50%, which should mimic a  
12 WS deletion. Thus, transcriptional consequences of hemizyosity of this gene might  
13 be similarly small.

14

15 *Frameshift mutation is sufficient to affect behavior*

16

17 Although we observed only small differences in DNA binding and overall  
18 brain transcription, another *Gtf2ird1* model also reported little to no effects of  
19 mutation on transcriptome-wide expression in the brain, yet the model still showed  
20 behavioral phenotypes (8,34). Therefore, we tested our mutation for downstream  
21 consequences on adult mouse behavior (**Table 1**). There are many single gene  
22 knockout models of *Gtf2ird1* and each shows distinct behavioral differences which  
23 are, in some instances, contradictory (8,9,21,35). One consistent phenotype across

1 models is a deficit in motor coordination, which is also affected in individuals with  
2 WS. Similarly, we observed a significant effect of genotype ( $H_2=16.35$ ,  $p=0.0003$ ), on  
3 balance. Heterozygous and homozygous animals fell off a ledge sooner than WT  
4 littermates ( $p=0.0038$ ,  $p=0.0007$ , respectively) (**Figure 5A**). Marble burying has not  
5 been reported in other *Gtf2ird1* models, but in larger WS models that delete the  
6 entire syntenic WSCR or the proximal half of the region containing *Gtf2ird1* have  
7 shown decreased marble burying in mutants (5,36). We observed a similar  
8 significant effect of genotype on the number of marbles buried ( $F_{2,80}=6.17$ ,  $p$   
9  $=0.0033$ ), with *Gtf2ird1*<sup>-/-</sup> mutants burying fewer marbles than WT mice ( $p=0.002$ )  
10 (**Figure 5B**). Reports of overall activity levels in *Gtf2ird1* mouse models have been  
11 discrepant (9,21). Here we show there is no main effect of genotype ( $F_{2,88}=1.36$ ,  
12  $p=0.263$ ) but a time by genotype interaction ( $F_{10,440}=5.791$ ,  $p=3.3\times 10^{-8}$ ) on total  
13 distance traveled in a one-hour locomotor task. Though no single time point showed  
14 a difference between genotypes when performing post hoc tests, this may reflect an  
15 overall difference in habituation to the chamber (**Figure 5C**). When taking sex into  
16 consideration, there was a main effect of sex ( $F_{1,85}=5.23$ ,  $p=0.025$ ) and the genotype  
17 by time interaction persists ( $F_{10,425}=5.82$ ,  $p=3.06\times 10^{-8}$ ) (**Supplemental Figure 3**  
18 **A,B**). Time spent in the center of an open field is used as a measure of anxiety-like  
19 behavior in mice. Anxiety-like behaviors in *Gtf2ird1* models have also been  
20 discrepant in the literature (8). Here we show that there was no main effect of  
21 genotype on center variables in this task ( $F_{2,88}=0.88$ ,  $p=0.42$ ) (**Figure 5D**).

22 Finally, as individuals with WBS also show a high prevalence of phobias,  
23 sensitivity to sounds, and learning deficits (3,37), we tested sensory motor gating



1 and learning and memory. Pre-pulse inhibition (PPI) results from a decreased  
2 startle to an auditory stimulus when the startle stimulus is preceded by a smaller  
3 stimulus. PPI was reduced in animals with the proximal WSCR region deleted, but  
4 mice with the distal deletion or full deletion did not have any abnormal phenotype  
5 (6). In our study, there was no main effect of genotype on PPI ( $F_{2,87}=0.24$ ,  $p=0.79$ ),  
6 but a pre-pulse by genotype interaction ( $F_{4,174}=2.66$ ,  $p=0.034$ ), which suggests that  
7 for some pre-pulse stimuli there is a difference between mutants and WT  
8 littermates, however no comparisons survived multiple testing corrections in the  
9 post hoc test (**Figure 5E**).

10 In our assessment of learning and memory with the conditioned fear  
11 paradigm, there was a main effect of genotype ( $F_{2,83}=4.82$ ,  $p=0.010$ ) and minute  
12 ( $F_{1,83}=9.75$ ,  $p=0.002$ ) on baseline freezing. Post hoc tests on baseline data showed  
13 the heterozygous mutants froze more than homozygous mutants during minute one  
14 ( $p=0.0065$ ). After the baseline, when animals were trained to associate a tone with a  
15 footshock, we observed all mice had increased freezing over time ( $F_{2,122}=26.77$ ,  
16  $p=2.28 \times 10^{-10}$ ) as expected. (**Figure 5E**). On the second day, which tested contextual  
17 fear memory, all genotypes exhibited a fear memory response as indicated by the  
18 significant effect of the context compared to baseline ( $F_{1,83}=173.20$ ,  $p < 2 \times 10^{-16}$ ). Each  
19 group froze more during the first two minutes of day two than on day one (WT:  
20  $p=1.98 \times 10^{-8}$ , *Gtf2ird1*<sup>+/-</sup>:  $p=4.97 \times 10^{-11}$ , *Gtf2ird1*<sup>-/-</sup>:  $p < 2 \times 10^{-16}$ ) (**Supplemental Figure**  
21 **3C**). When we analyzed the entire time of the experiment of contextual fear we  
22 similarly saw no main effect of genotype ( $F_{2,83}=2.8946$ ,  $p=0.061$ ), but a significant  
23 effect of time ( $F_{7,581}=15.05$ ,  $p < 2 \times 10^{-16}$ ) and a time by genotype interaction

1 ( $F_{14,581}=2.01$ ,  $p=0.016$ ). Post hoc analysis showed that during minute two the  
2 homozygous animals froze significantly more than the *Gtf2ird1*<sup>+/-</sup> mutants  
3 ( $p=0.026$ ). Similarly, the homozygous mutants froze more than WT littermates  
4 during minutes two ( $p=0.021$ ) and three ( $p=0.012$ ), suggesting an increased  
5 contextual fear memory response (**Figure 5G**). On day three of the experiment, we  
6 tested cued fear. During day three baseline we saw a difference in freezing between  
7 genotypes ( $F_{2,83}=4.13$ ,  $p=0.02$ ) as well as a time by genotype interaction ( $F_{2,83}=4.47$ ,  
8  $p=0.014$ ), with homozygous mutants freezing more in minute two than WT  
9 littermates ( $p=0.002$ ). All genotypes had a similar response to the tone ( $F_{2,83}=0.36$ ,  
10  $p=0.70$ ) (**Figure 5H**). These differences could not be explained by differences in  
11 shock sensitivity (flinch:  $H_2=2.52$ ,  $p=0.28$ , escape:  $H_2=3.13$ ,  $p=0.21$ , vocalization:  
12  $H_2=2.20$ ,  $p=0.33$ ) (**Supplemental Figure 3D**). Thus, mutation of *Gtf2ird1* appears to  
13 enhance contextual fear learning.

14 Overall, these behavioral analyses show the N-terminal truncation and/or  
15 decreased protein levels of the *Gtf2ird1* mutant still result in adult behavioral  
16 phenotypes, specifically in the domains of balance, marble burying, and fear  
17 conditioning. The most severe phenotypes were observed in the homozygous  
18 mutants, which may model the haploinsufficiency of WS deletions.

19

20 *Generation of a Gtf2i and Gtf2ird1 double mutant*

21

22 The evidence of functional consequences from the one base pair *Gtf2ird1*  
23 frameshift mutation led us to characterize a double mutant that was generated

1 during the dual gRNA CRISPR/Cas9 injections. This mutant allowed us to test the  
2 effects of knocking out *Gtf2i* combined with a *Gtf2ird1* mutation, and test different  
3 *Gtf2ird1* mutations for consistency in phenotypes. The double mutant described  
4 here has a two base pair deletion in exon five of *Gtf2i* and a 590bp deletion that  
5 encompasses most of exon three of *Gtf2ird1* (**Figure 6A**). We carried out a  
6 heterozygous cross of the double mutants to test the protein and transcript  
7 abundance of each gene in the heterozygous and homozygous states. The  
8 homozygous double mutant is embryonic lethal due to the lack of *Gtf2i*, which has  
9 been described in other *Gtf2i* mutants (**Figure 6B**) (4,38). We were, however, able  
10 to detect homozygous embryos up to E15.5. Thus, we focused molecular analyses on  
11 E13.5 brains. The two base pair deletion in exon five of *Gtf2i* leads to a premature  
12 stop codon resulting in a full protein knockout, and decreases the transcript  
13 abundance consistent with degradation of the mRNA due to nonsense-mediated  
14 decay (**Figure 6C,D**). The 590bp deletion in *Gtf2ird1* removes all of exon three  
15 except the first 14bp. We observed the same increase in transcript abundance that  
16 was detected in the one base pair insertion mutation but this mutation had a larger  
17  
18 effect on protein levels across genotype, with homozygous mutants producing a  
19 truncated protein at about 10% of WT levels (**Figure 6E,F**).

20

21 *Knocking down both Gtf2i and Gtf2ird1 produces mild transcriptomic changes*

22

1 To test if combined mutation of *Gtf2i* and *Gtf2ird1* had a larger effect on the  
2 transcriptome, we performed whole brain RNA-seq analysis on WT E13.5 brains  
3 and compared them to *Gtf2i*<sup>+/-</sup>/*Gtf2ird1*<sup>+/-</sup> littermates. Similar to what was seen in  
4 the previous *Gtf2ird1*<sup>-/-</sup> mutants, there were only mild differences between the  
5 transcriptomes (**Figure 6G**). We also compared WT transcriptomes to the  
6 homozygous double mutants, which showed greater differences. However, since  
7 these mutants have a very severe phenotype, including neural tube closure defects,  
8 any direct transcriptional consequences are probably masked by a large number of  
9 indirect effects. Indeed, GO term analysis suggested that overall nervous system  
10 development and glial cell differentiation is disrupted (**Supplemental Figure 4A,B**).  
11 We also analyzed GTF2I ChIP-seq data with RNA-seq data. Unlike the enriched  
12 binding at highly expressed genes we saw with GTF2IRD1 alone, gene expression  
13 levels were not significantly related to GTF2I binding ( $\chi^2 = 6.58$ , d.f.=3 p=0.086)  
14 (**Figure 6H**). This is consistent with a previous report of GTF2I ChIP-seq data.  
15 Again, the majority (963 peaks) of the TSS GTF2I peaks were nearby expressed  
16 genes, with 458 next to genes not expressed at detectable levels in the E13.5 brain.  
17 There is a slight but significant increase in gene expression of genes bound by GTF2I  
18 compared to genes that are not (0.0213 logFC, Kolmogorov-Smirnov test D=0.075,  
19 p=9.50x10<sup>-5</sup>) (**Figure 6I**). Thus, heterozygous *Gtf2i* and *Gtf2ird1* mutation, like  
20 *Gtf2ird1* mutation alone, results in very subtle transcriptional changes.

21 *Double mutants show behavioral consequences similar to single Gtf2ird1 mutants*

22

1 To test the effects of mutating both *Gtf2i* and *Gtf2ird1* on behavior, we  
2 crossed the heterozygous double mutant to the single *Gtf2ird1* heterozygous mouse  
3 (**Figure 7A**). This breeding strategy produced four littermate genotypes, WT,  
4 *Gtf2ird1*<sup>+/-</sup>, *Gtf2i*<sup>+/-</sup>/*Gtf2ird1*<sup>+/-</sup>, and *Gtf2i*<sup>+/-</sup>/*Gtf2ird1*<sup>-/-</sup> for direct and well-controlled  
5 comparisons. To test for additive effects, the primary comparison was contrasting  
6 *Gtf2ird1*<sup>+/-</sup> mice to *Gtf2i*<sup>+/-</sup>/*Gtf2ird1*<sup>+/-</sup> littermates. The remaining genotype, *Gtf2i*<sup>+/-</sup>  
7 /*Gtf2ird1*<sup>-/-</sup>, further tested the effects of heterozygous *Gtf2i* mutation in the presence  
8 of both *Gtf2ird1* mutations. To be thorough, we tested protein and transcript  
9 abundance of each gene in all four genotypes. As expected, all genotypes with the  
10 *Gtf2i* mutation showed decreased protein and transcript levels. The *Gtf2ird1* results  
11 reflected what was previously shown for each mutation, however, *Gtf2i*<sup>+/-</sup>/*Gtf2ird1*<sup>-/-</sup>  
12 did not show any further detectable decrease in protein abundance compared to the  
13 *Gtf2i*<sup>+/-</sup>/*Gtf2ird1*<sup>+/-</sup> genotype (**Supplemental Figure 5A-D**), with both at about 50%  
14 of WT levels.

15 We repeated the same behaviors performed on the one base pair *Gtf2ird1*  
16 mutants (**Table 2**). We saw a similar significant effect of genotype on balance  
17 ( $H_3=10.68$ ,  $p=0.014$ ), with *Gtf2i*<sup>+/-</sup>/*Gtf2ird1*<sup>-/-</sup> mice falling off sooner compared to WT  
18 littermates ( $p=0.025$ ) (**Figure 7B**). There was no significant difference between the  
19 *Gtf2ird1*<sup>+/-</sup> and *Gtf2i*<sup>+/-</sup>/*Gtf2ird1*<sup>+/-</sup> genotypes, suggesting that decreasing the dosage  
20 of GTF2I does not strongly modify the *Gtf2ird1*<sup>+/-</sup> phenotype. There was a significant  
21 effect of genotype on the number of marbles buried ( $F_{3,76}=2.93$ ,  $p=0.039$ ). Post hoc  
22 analysis showed a significant difference between only *Gtf2ird1*<sup>+/-</sup> and *Gtf2i*<sup>+/-</sup>  
23 /*Gtf2ird1*<sup>-/-</sup> littermates ( $p=0.050$ ) (**Figure 7C**), with a trend in the same direction as

1 was previously seen in the *Gtf2ird1*<sup>-/-</sup> mutants. We saw a main effect of genotype on  
2 activity levels in the one-hour locomotor task ( $F_{3,69}=3.22$ ,  $p=0.028$ ), but we did not  
3 see the same main effect of sex ( $F_{1,69}=2.29$ ,  $p=0.14$ ), or a sex by genotype interaction  
4 ( $F_{3,69}=1.82$ ,  $p=0.15$ ); however we did see a three-way sex by time by genotype  
5 interaction ( $F_{15,345}=1.95$ ,  $p=0.018$ ). The combined sex data showed *Gtf2i*<sup>+/-</sup>/*Gtf2ird1*<sup>-/-</sup>  
6 mice travel a greater distance than WT and *Gtf2ird1*<sup>+/-</sup> mice at time point 40  
7 (**Figure 7D**). When we looked at the data by sex, we saw a larger effect in females  
8 with *Gtf2ird1*<sup>+/-</sup> and *Gtf2i*<sup>+/-</sup>/*Gtf2ird1*<sup>+/-</sup> genotypes intermediate to *Gtf2i*<sup>+/-</sup>/*Gtf2ird1*<sup>-/-</sup>  
9 (**Supplemental Figure 5E,F**). There was also a main effect of genotype on the time  
10 spent in the center of the apparatus ( $F_{3,69}=3.60$ ,  $p=0.018$ ) that was not seen in the  
11 previous *Gtf2ird1* cross. *Gtf2i*<sup>+/-</sup>/*Gtf2ird1*<sup>-/-</sup> mice spent less time in the center during  
12 the first ten minutes of the task compared to WTs ( $p=0.0019$ ) (**Figure 7E**).

13 Finally, we repeated the PPI and conditioned fear memory tasks using this  
14 breeding strategy. In contrast to what was observed for PPI in the *Gtf2ird1* cross, we  
15 saw a significant main effect of genotype ( $F_{3,84}=4.59$ ,  $p=0.0051$ ). The *Gtf2i*<sup>+/-</sup>/  
16 *Gtf2ird1*<sup>-/-</sup> mice showed an attenuated PPI response especially at the louder pre-  
17 pulse stimuli compared to WT littermates (PPI8: $p=0.02$ , PPI16: $p=0.018$ ) and  
18 *Gtf2ird1*<sup>+/-</sup> mice (PPI16: $p=0.02$ ) (**Figure 7F**). On day one of the conditioned fear  
19 task, all genotypes showed increased freezing with subsequent foot shocks as  
20 expected. WT animals exhibited higher freezing during minute one of baseline, but  
21 this difference diminished during minute two (**Figure 7G**). All animals showed a  
22 contextual fear memory response when they were re-introduced to the chamber on  
23 day two ( $F_{1,68}=81.21$ ,  $p=3.21 \times 10^{-13}$ ) (**Supplemental Figure 5G**). While there was no

1 main effect of genotype ( $F_{3,68}=1.61$ ,  $p=0.19$ ) (**Figure 7H**), the *Gtf2ird1*<sup>+/-</sup> and double  
2 mutants showed a trend towards increased freezing that was seen in the previous  
3 behavior cohort. On day three, when cued fear was tested, there was a significant  
4 effect of genotype on the freezing behavior ( $F_{3,68}=3.17$ ,  $p=0.030$ ) and a time by  
5 genotype interaction ( $F_{21,476}=1.63$ ,  $p=0.040$ ). During minute five of the task the  
6 *Gtf2i*<sup>+/-</sup>/*Gtf2ird1*<sup>-/-</sup> mutants froze significantly more than WTs ( $p=0.030$ ) as did the  
7 *Gtf2ird1*<sup>+/-</sup> ( $p=0.024$ ) (**Figure 7I**). The cued fear phenotype could not be explained  
8 by differences in shock sensitivity (**Supplemental Figure 5H**).

9 By crossing these mutant lines, we tested the hypothesis that the double  
10 heterozygous mutant would be more severe than a mutation only affecting *Gtf2ird1*.  
11 *Gtf2ird1*<sup>+/-</sup> and *Gtf2i*<sup>+/-</sup>/*Gtf2ird1*<sup>+/-</sup> genotypes resulted in mild deficits compared to  
12 WTs that, in some cases, were intermediate to the *Gtf2i*<sup>+/-</sup>/*Gtf2ird1*<sup>-/-</sup> phenotype.  
13 There were no instances where the *Gtf2ird1*<sup>+/-</sup> or *Gtf2i*<sup>+/-</sup>/*Gtf2ird1*<sup>+/-</sup> genotypes were  
14 significantly different from each other, suggesting that in the behaviors we have  
15 tested, the *Gtf2i* mutation does not modify the effects of a *Gtf2ird1* mutation. This  
16 unique cross also allowed us to characterize a new mouse line *Gtf2i*<sup>+/-</sup>/*Gtf2ird1*<sup>-/-</sup>,  
17 which had the largest impact on behaviors. The phenotypes of *Gtf2i*<sup>+/-</sup>/*Gtf2ird1*<sup>-/-</sup>  
18 were always in the same direction as the phenotypes in the *Gtf2ird1*<sup>-/-</sup> mouse model,  
19 but we also saw a significant PPI deficit and cued fear difference when the *Gtf2i*  
20 mutation was added. This further supports that the behaviors tested here, such as,  
21 balance, marble burying, and learning and memory are largely affected by  
22 homozygous mutations in *Gtf2ird1*.

23

## 1 **Discussion**

2           We have described the *in vivo* DNA binding sites of GTF2IRD1 and GTF2I in  
3 the developing mouse brain. This is the first description of these two transcription  
4 factors in a tissue that is relevant for the behavioral phenotypes seen in mouse  
5 models of WS. GTF2IRD1 showed a preference for active sites and promoter regions.  
6 The conservation of GTF2IRD1 targets was higher on average than would be  
7 expected by chance, which provides evidence that these are functionally important  
8 regions of the genome. The functions of genes bound by GTF2IRD1 include  
9 transcriptional regulation, such as chromatin modifiers, as well as post-translational  
10 regulation including protein ubiquitination. A role for GTF2IRD1 in regulating genes  
11 involved in protein ubiquitination has not been described before. This supports the  
12 role of GTF2IRD1 in regulating chromatin by transcriptionally controlling other  
13 chromatin modifiers. These data, along with the localization pattern of GTF2IRD1 in  
14 the nucleus and its direct association with other chromatin modifiers such as  
15 ZMYM5 (18,39), suggests that GTF2IRD1 can exert its regulation of chromatin at  
16 several different levels of biological organization. Motif enrichment analysis of  
17 GTF2IRD1 peaks indicated that CTCF cobind with GTF2IRD1. Consistent with this,  
18 GTF2IRD1 is also often present at TAD boundaries where CTCF is known to be  
19 enriched. This further suggests GTF2IRD1 may have a role in defining chromatin  
20 topology. GTF2I has been shown to interact with and target CTCF to specific sites in  
21 the genome (25) so it would be interesting to test if GTF2IRD1 has a similar  
22 relationship with CTCF.



1 Overall, GTF2I showed a similar preference for promoters and active regions,  
2 although it had more intergenic targets than GTF2IRD1, and the conservation of  
3 GTF2I peaks was significantly lower than GTF2IRD1 peaks. The genes bound by  
4 GTF2I were enriched for signal transduction and phosphorylation. Interestingly,  
5 GTF2I was bound to the *Src* gene body . SRC is known to phosphorylate GTF2I to  
6 induce its transcriptional activity (16). Phosphorylation of GTF2I by SRC also  
7 antagonizes calcium entry into the cell (17). While knocking out *Gtf2i* did not affect  
8 the expression of *Src*, it would be interesting to understand the functional  
9 consequence of GTF2I binding *Src*, especially since *Src* knockout mice exhibit similar  
10 behaviors as *Gtf2i* mouse models (40).

11 The overlap of GTF2I and GTF2IRD1 targets was significant, and the target  
12 genes were enriched for synaptic activity and signal transduction. This is evidence  
13 that these genes can interact via their binding targets to produce cognitive and  
14 behavioral phenotypes. To test the difference between combined *Gtf2i* and *Gtf2ird1*  
15 mutation and mutation of *Gtf2ird1* alone, we characterized two new mouse models.  
16 We used the CRISPR/Cas9 system to generate multiple mutations in the two genes  
17 individually as well as together from one embryo injection. The ease and  
18 combinatorial possibilities of this technology will be amenable to testing many  
19 unique combinations of genetic mutations in copy number variant regions, which  
20 will be important to fully understand the complex relationships of genes in these  
21 disorders.

22 We found a frameshift mutation expected to trigger non-sense mediated  
23 decay in *Gtf2ird1* did not degrade the mRNA but did result in an N-terminal

1 truncation and protein level reduction in the homozygous mutant (23). Even a  
2 larger, 590bp deletion of exon three in *Gtf2ird1* did not result in mRNA degradation,  
3 but did have a larger effect on protein level. This phenomenon of increased *Gtf2ird1*  
4 RNA levels has been seen in at least three other mouse models of *Gtf2ird1* (8,23,32).  
5 Two of these were made using classic homologous recombination removing either  
6 exon two alone or exon two through part of exon five. In both of these models,  
7 *Gtf2ird1* transcript was still made, but no *in vivo* protein analysis was done due to  
8 poor quality antibodies and the undetectably low protein expression in WT mice.  
9 The third model also saw the N-terminal truncation. The presence of an aberrant  
10 protein that can still bind the genome, such as the mutant described here, could  
11 explain the lack of transcriptomic differences in the brain shown here and by others  
12 (34). The mutant protein may also still interact with other binding partners and be  
13 trafficked to the appropriate genomic loci. This mutation did disrupt the binding of  
14 GTF2IRD1 to its own promoter, which resulted in an increase in transcript levels.  
15 The property that specifies GTF2IRD1 binding to its own promoter must be unique,  
16 as DNA binding genome-wide was not robustly perturbed in the mutant.

17 In the end, GTF2IRD1 has proven to be a remarkably difficult protein to  
18 disrupt in a targeted manner – a finding that may modify interpretation of prior  
19 studies using a variety of mutant lines, including ours (23). Indeed, it took years to  
20 establish a sufficiently sensitive immunoblotting protocol for GTF2IRD1, much less a  
21 ChIP-seq protocol to study its binding genome wide. Thus, even in the current study,  
22 much of the transcriptional and behavioral characterization was complete prior to  
23 discovering that substantial DNA binding remained. Presumably the resiliency of

1 this binding also extends to the mutants we used in our recent test of the sufficiency  
2 of Gtf2i family mutants to recapitulate the deletion of the entire locus (23).  
3 Therefore, it remains challenging to determine to what extent existing *Gtf2ird1*  
4 exonic mutants model the loss of this gene in WS, where the whole genic locus is  
5 deleted. Interestingly, when the whole locus is deleted in the “CD” complete  
6 deletion mice, the elevation of *Gtf2ird1* mRNA seen in exonic mutants does not occur  
7 (23). However, protein levels appear to stay above 50%, albeit with substantial  
8 mouse to mouse variation. Post-mortem patient brain samples, if available, may  
9 help to resolve the consequences of the human mutation on GTF2IRD1 protein  
10 levels. Further, it may be worth revisiting the consequences of *Gtf2ird1* mutation  
11 following generation of full genic deletions in mice. In the meantime, it may be that  
12 some of the homozygous point mutations, though different from the heterozygous  
13 mutations of WS, may better model WS protein levels as they can result in a  
14 reduction of GTF2IRD1 protein (**Figure 4**). Indeed, most studies of *Gtf2ird1* mutant  
15 behavioral consequences have shown atypical phenotypes in homozygous mutant  
16 mice (8,9,21).

17 It is worth noting that even in those mutants with a 50% reduction in  
18 protein, transcriptional changes are very subtle, at least at steady state. This is  
19 similar to findings in other chromatin modifying knockouts, where final changes in  
20 transcription are highly subtle (41–45), even when behavioral consequences can be  
21 severe or even lethal, in the case of *Mecp2* mutants Guy et al. Nat Gen. 2001 (46).  
22 Thus, a second remaining puzzle about these genes is what their role is in regulating  
23 transcription at the majority of their binding sites. One possibility is these genes are

1 essential for regulating the proper dynamics of gene expression, something not  
2 captured when assessing a population at steady state. Another possibility is they  
3 affect phenotypes via actions in rare cell types not easily detected in whole brain  
4 RNA-seq. Both hypotheses await further experimentation. Nonetheless, the strong  
5 enrichment of ASD and constrained genes among GTF2I and especially GTF2IRD1  
6 targets suggest that these factors may be key regulators. Such functional  
7 interactions suggest common pathways across these chromatin-related forms of  
8 ASD and intellectual disability.

9       Regardless of the resiliency at the protein level, we show heterozygous and  
10 homozygous mutations of *Gtf2ird1* were sufficient to cause adult behavioral  
11 abnormalities. This supports the hypothesis that the N-terminal end of the protein  
12 has other important functions beyond DNA binding. Similarly, the N-truncation of  
13 GTF2I did not affect DNA-binding genome-wide, but still resulted in behavioral  
14 deficits (47). The single *Gtf2ird1* homozygous mutant showed balance deficits,  
15 which is consistent across many mouse models of WS. We also observed decreased  
16 marble burying. This task is thought to be mediated at least in part by hippocampal  
17 function, suggesting a possible disruption of the hippocampus caused by this  
18 mutation (48). We also observed an increase in contextual fear response, another  
19 cognitive task that is thought to be under hippocampal and amygdalar regulation.  
20 Increase in contextual fear was also seen in another *Gtf2ird1* mouse model (49).

21       Given the prior evidence that these two transcription factors are both  
22 involved in cognitive and behavioral phenotypes of WS (7,50), and the evidence that  
23 their shared binding targets regulate synaptic genes, we tested if having both *Gtf2i*

1 and *Gtf2ird1* mutated could modify the phenotype seen when just *Gtf2ird1* was  
2 mutated. Contrary to our prediction, we did not see a large effect of adding a *Gtf2i*  
3 mutation to differences in transcriptome wide expression or behavioral phenotypes.  
4 This was also surprising given that we successfully reduced GTF2I protein and it has  
5 been described in the literature as regulating transcription (51). Again, whole E13.5  
6 brain analysis could diminish any effects of transcriptional differences in specific  
7 cell types. This potential confound could be overcome using single cell sequencing  
8 technologies in the future when those technologies mature and become more  
9 reliable for detecting within cell type differences of expression.

10       When *Gtf2i* was knocked down in the presence of two *Gtf2ird1* mutations, we  
11 saw phenotypes in the same direction as the homozygous one base pair insertion  
12 *Gtf2ird1* mutant, as well as significant increases in the cued fear memory task. Thus,  
13 the behaviors tested in this study seem to be mainly driven by *Gtf2ird1* mutant  
14 homozygosity, which is consistent across the different mutations. The one exception  
15 seemed to be PPI, in which the knockdown of *Gtf2i* in the presence of two *Gtf2ird1*  
16 mutations attenuated the effect of the pre-pulse. There was no effect of homozygous  
17 *Gtf2ird1* mutation alone on this phenotype, suggesting that *Gtf2i* and not *Gtf2ird1* is  
18 playing a larger role. However, the more severe phenotype was seen in the *Gtf2i*<sup>+/-</sup>  
19 */Gtf2ird1*<sup>-/-</sup> mutant compared to *Gtf2i*<sup>+/-</sup>*/Gtf2ird1*<sup>+/-</sup>, suggesting a contribution from  
20 both genes. This does not exclude the possibility that *Gtf2i* can modify the  
21 phenotype of *Gtf2ird1* knockdown in other behavioral domains. For example, it  
22 would be interesting to see the effect of adding a *Gtf2i* mutation on top of a *Gtf2ird1*  
23 mutation on social behaviors. However, on the FVB/AntJ background used here and

1 in F1 FVB/AntJ x C57BL/6J crosses used previously, we have not seen any social  
2 behavior disruptions when these genes are mutated or the entire WS locus is  
3 deleted (23).

4 Likewise, the fear conditioning effects of even heterozygous *Gtf2ird1*  
5 mutation are very clear on the FVB/AntJ background used here, but appear to be  
6 masked in F1 FVB x C57BL/6J crosses used in our prior study (23). This indicates  
7 that while we did not find evidence for epistasis between *Gtf2i* and *Gtf2ird1*, there is  
8 epistasis between these genes and other loci in the genome. Thus, mouse mapping  
9 studies using large cohorts of F2 hybrids might provide an opportunity to leverage  
10 this strain difference to find genes that interact with *Gtf2ird1* to contribute to these  
11 phenotypes. Such studies could help define novel interaction partners for this  
12 relatively understudied gene.

13 Overall, our study has provided the first description of the DNA-binding of  
14 both GTF2I and GTF2IRD1 in the developing mouse brain and showed they have  
15 unique and overlapping targets. These data will be used to inform downstream  
16 studies to understand how these transcription factors interact with the genome. We  
17 generated two new mouse models that tested the importance of the N-terminal end  
18 of GTF2IRD1 and the effect of mutating both *Gtf2i* and *Gtf2ird1* together. We  
19 provided evidence that despite neither gene having much effect on transcription, the  
20 *Gtf2ird1* mutation affects balance, marble burying, activity levels and fear memory  
21 while adding a *Gtf2i* mutation leads to a larger effect on PPI.

22

23 **Materials and Methods**

1 *Generating genome edited mice*

2

3 We generated *Gtf2i* family mutants as described in (23). To generate unique  
4 combinations of gene knockouts, we designed gRNAs targeting early constitutive  
5 exons of the mouse *Gtf2i* and *Gtf2ird1* genes. The gRNAs were separately cloned into  
6 the pX330 Cas9 expression plasmid (a gift from F. Zhang) and transfected in N2a  
7 cells to test for cutting efficiency. DNA was harvested from the cells and cutting was  
8 detected using the T7 endonuclease assay. The gRNAs were transcribed *in vitro*  
9 using the MEGAShortScript kit (Ambion, Austin, TX) and the Cas9 mRNA was *in vitro*  
10 transcribed using the mMessageMachine kit (Ambion). The two gRNAs and Cas9  
11 mRNA were injected into FVB/NJ mouse embryos and implanted into donor  
12 females. The resulting offspring were genotyped for mutations with gene specific  
13 primers designed with the Illumina adapter sequences concatenated to their 3'  
14 prime end to allow for deep sequencing of the amplicons surrounding the expected  
15 cut sites. In one line, a large 590 bp deletion in *Gtf2ird1* was detected by amplifying  
16 3.5kb that included exon two, exon three and part of intron three, then using a  
17 Nextera library prep (Illumina, San Diego, CA) to deep sequence the amplicon. Here  
18 we focus on two founder mice obtained from these injections. Founder lines were  
19 bred to FVB/AntJ mice to ensure the mutations existed in the germline and, for  
20 double mutant founders, on the same chromosome. The mice were further back-  
21 crossed until the mutations were on a complete FVB/AntJ background, which differs  
22 from the FVB/NJ background at two loci: *Tyr<sup>c-ch</sup>*, which gives FVB/AntJ a chinchilla  
23 coat color, and the 129P2/OlaHSd wildtype (WT) *Pde6b* allele, which prevents

1 FVB/AntJ from becoming blind in adulthood. Coat color was identified by eye, and  
2 the *Pde6b* gene was genotyped by PCR. These mouse lines are available through the  
3 MMRRC (accession numbers pending).

4

#### 5 *Western blotting*

6

7 Embryos were harvested on embryonic day 13.5 (E13.5) and the whole brain was  
8 dissected in cold PBS then flash frozen in liquid nitrogen. The brains were stored at -  
9 80°C until they were lysed. The frozen brain was homogenized in 500ul of 1xRIPA  
10 buffer (10mM Tris HCl pH 7.5, 140mM NaCl, 1mM EDTA, 1% Triton X-100, 0.1%  
11 DOC, 0.1% SDS, 10mM Na<sub>3</sub>V0<sub>4</sub>, 10mM NaF, 1x protease inhibitor (Roche, Basil,  
12 Switzerland)) along with 1:1000 dilution of RNase inhibitors (RNasin (Promega,  
13 Madison, WI) and SUPERase In (Thermo Fisher Scientific, Waltham, MA). The  
14 homogenate was incubated on ice for 20 minutes then spun at 10,000g for 10  
15 minutes at 4°C to clear the lysate. The lysate was stored in two aliquots of 100µl at -  
16 80°C for later protein analysis and 250µl of the lysate was added to 750µl of TRIzol  
17 LS and stored at -80°C for later RNA extraction and qPCR. Total protein was  
18 quantified using the BCA assay and 25-50µg of protein in 1x Lamelli Buffer with β-  
19 mercaptoethanol was loaded onto 4-15% TGX protean gels (Bio-Rad, Hercules, CA).  
20 The protein was transferred to a .2µm PVDF membrane by wet transfer. The  
21 membrane was blocked with 5% milk in TBST for one hour at room temperature.  
22 The membrane was cut at the 75KDa protein marker; the bottom was probed with a  
23 GAPDH antibody as an endogenous loading control, while the top was probed with



1 an antibody for either GTF2I or GTF2IRD1. The primary incubation was performed  
2 overnight at 4°C. The membrane was washed three times in TBST for five minutes,  
3 then incubated with an HRP conjugated secondary antibody diluted in 5% milk in  
4 TBST for one hour at room temperature. The blot was washed three times with  
5 TBST for five minutes then incubated with Clarity Western ECL substrate (Bio-Rad)  
6 for five minutes. The blot was imaged in a MyECL Imager (Thermo Fisher Scientific).  
7 Relative protein abundance was quantified using Fiji (NIH) and normalized to  
8 GAPDH levels in a reference WT sample. The antibodies used were: Rabbit anti-  
9 GTF2IRD1 (1:500, Novus, NBP1-91973), Mouse anti-GTF2I (1:1000 BD  
10 Transduction Laboratories, Lexington, KY, BAP-135), and Mouse anti-GAPDH  
11 (1:10,000, Sigma Aldrich, St. Louis, MO G8795), HRP-conjugated Goat anti Rabbit-  
12 IgG (1:2000, Sigma Aldrich, AP307P) and HRP-conjugated Goat anti-Mouse IgG  
13 (1:2000, Bio-Rad, 1706516).

14

#### 15 *Transcript abundance using RT-qPCR*

16

17 RNA was extracted from TRIzol LS using the Zymo Clean and Concentrator-5 kit  
18 with on column DNase-I digestion following the manufacturer's instructions. The  
19 RNA was eluted in 30µl of RNase free water and quantified using a Nanodrop 2000  
20 (Thermo Fisher Scientific). One microgram of RNA was transcribed into cDNA using  
21 the qScript cDNA synthesis kit (Quanta Biosciences, Beverly, MA). Half a microliter  
22 of cDNA was used in a 10µl PCR reaction with 500nM of target specific primers and  
23 the PowerUP SYBR green master mix (Applied Biosystems, Foster City, CA). The

1 primers were designed to amplify exons that were constitutively expressed in both  
2 *Gtf2i* (exons 25 and 27) and *Gtf2ird1* (exons 8 and 9) and span an intron (23). The  
3 RT-qPCR was carried out in a QuantStudio6Flex machine (Applied Biosystems)  
4 using the following cycling conditions: 1) 95°C for 20 seconds, 2) 95°C for 1 second,  
5 3) 60°C for 20 seconds, then repeat steps 2 and 3 40 times. Each target and sample  
6 was run in triplicate technical replicates, with three biological replicates for each  
7 genotype. The relative transcript abundance was determined using the delta CT  
8 method normalizing to *Gapdh*.

9

#### 10 *ChIP*

11

12 Chromatin was prepared as described previously (23). Frozen brains were  
13 homogenized in 10mL of cross-linking buffer (10mM HEPES pH7.5, 100mM NaCl,  
14 1mM EDTA, 1mM EGTA, 1% Formaldehyde (Sigma Aldrich)). The homogenate was  
15 spun down and resuspended in 5mL of 1x L1 buffer (50mM HEPES pH 7.5, 140 mM  
16 NaCl, 1mM EDTA, 1mM EGTA, 0.25% Triton X-100, 0.5% NP40, 10.0% glycerol,  
17 1mM BGP (Sigma Aldrich), 1x Na Butyrate (Millipore, Burlington, MA), 20mM NaF,  
18 1x protease inhibitor (Roche)) to release the nuclei. The nuclei were spun down and  
19 resuspended in 5mL of L2 buffer (10mM Tris-HCl pH 8.0, 200mM NaCl, 1mM BGP,  
20 1x Na Butyrate, 20mM NaF, 1x protease inhibitor) and rocked at room temperature  
21 for five minutes. The nuclei were spun down and resuspended in 950µl of buffer L3  
22 (10mM Tris-HCl pH 8.0, 1mM EDTA, 1mM EGTA, 0.3% SDS, 1mM BGP, 1x Na  
23 Butyrate, 20mM NaF, 1x protease inhibitor) and sonicated to a fragment size of 100-

1 500bp in a Covaris E220 focused-ultrasonicator with 5% duty factor, 140 PIP, and  
2 200cbp. The sonicated chromatin was diluted with 950ul of L3 buffer and 950µl of  
3 3x Covaris buffer (20mM Tris-HCl pH 8.0, 3.0% Triton X-100, 450mM NaCl, 3mM  
4 EDTA). The diluted chromatin was pre-cleared using 15µl of protein G coated  
5 streptavidin magnetic beads (Thermo Fisher Scientific) for two hours at 4°C. For IP,  
6 15µl of protein G coated streptavidin beads were conjugated to either 10µl of  
7 GTF2IRD1 antibody (Rb anti-GTF2IRD1, NBP1-91973 LOT:R40410) or 10µl of  
8 GTF2I antibody (Rb anti-GTF2I, Bethyl Laboratories, Montgomery, TX, A301-330A)  
9 for one hour at room temperature. 80µl of the pre-cleared lysate was saved for an  
10 input sample. 400µl of the pre-cleared lysate was added to the beads and incubated  
11 overnight at 4°C. The IP sample was then washed twice with low salt wash buffer  
12 (10mM Tris-HCl pH 8.0, 2mM EDTA, 150mM NaCl, 1.0% Triton X-100, 0.1% SDS),  
13 twice with a high salt buffer (10mM Trish-HCl pH 8.0, 2mM EDTA, 500mM NaCl,  
14 1.0% Triton X-100, 0.1% SDS), twice with LiCl wash buffer (10mM Tris-HCl pH 8.0,  
15 1mM EDTA, 250mM LiCl (Sigma Aldrich), 0.5% NaDeoxycholate, 1.0% NP40), and  
16 once with TE buffer (10mM Tris-HCl pH 8.0, 1mM EDTA). The DNA was eluted from  
17 the beads with 200µl of 1x TE and 1% SDS by incubating at 65°C in an Eppendorf R  
18 thermomixer shaking at 1400rpm. The DNA was de-crosslinked by incubating at  
19 65°C for 15 hours in a thermocycler. RNA was removed by incubating with 10ug of  
20 RNase A (Invitrogen, Carlsbad, CA) at 37°C for 30 minutes and then treated with  
21 140ug of Proteinase K (NEB, Ipswich, MA) incubating at 55°C in a thermomixer  
22 mixing at 900rpm for two hours. The DNA was extracted with 200µl of  
23 phenol/chloroform/isoamyl alcohol (Ambion) and cleaned up using the Qiagen PCR

1 purification kit then eluted in 60ul of elution buffer. Concentration was assessed  
2 using the high sensitivity DNA kit for Qubit quantification (Thermo Fisher  
3 Scientific).

4

#### 5 *ChIP-qPCR*

6

7 Primers were designed to amplify the upstream regulatory element of *Gtf2ird1*. Two  
8 off target primers were designed: one 10kb upstream of the transcription start site  
9 of *Bdnf* and the other 7kb upstream of the *Pcbp3* transcription start site. The input  
10 sample was diluted 1:3, 1:30, and 1:300 to create a standard curve for each primer  
11 set and sample. Each standard, input, and IP sample for each primer set was  
12 performed in triplicate in 10µl reactions using the PowerUP SYBR green master mix  
13 (Applied Biosystems) and 250nM of forward and reverse primers. The reactions  
14 were performed in a QuantStudio6Flex machine (Applied Biosystems) with the  
15 following cycling conditions: 1) 50°C for 2 minutes, 2) 95°C for 10 minutes, 3) 95°C  
16 15 seconds, 4) 60°C for 1 minute, then repeat steps 3-4 40 times. The relative  
17 concentration of the input and IP samples were determined from the standard curve  
18 for each primer set. Enrichment of the IP samples was determined by dividing the  
19 on target upstream regulatory element relative concentration by the off target  
20 relative concentration.

21

#### 22 *ChIP-seq*

23

1 ChIP seq libraries were prepared using the Swift Accel-NGS 2S plus DNA library  
2 prep kits with dual indexing (Swift Biosciences, Ann Arbor, MI). The final libraries  
3 were enriched by 13 cycles of PCR. The libraries were sequenced by the Genome  
4 Technology Access Center at Washington University School of Medicine on a  
5 HiSeq3000 producing 1x50 reads.

6 Raw reads were trimmed of adapter sequences and bases with a quality  
7 score below 25 using the Trimmomatic Software (52). The trimmed reads were  
8 aligned to the mm10 genome using the default settings of bowtie2 (53). Reads with  
9 a mapping quality of less than 10 were removed. Picard tools was used to remove  
10 duplicates from the filtered reads (<http://broadinstitute.github.io/picard>). Macs2  
11 was used to call peaks on the WT IP, *Gtf2ird1*<sup>-/-</sup> IP, and *Gtf2i*<sup>-/-</sup>/*Gtf2ird1*<sup>-/-</sup> IP samples  
12 with the corresponding sample's input as the control for each biological replicate  
13 (54). Macs2 used an FDR of 0.01 as the threshold to call a significant peak. High  
14 confidence peaks were those peaks that had some overlap within each biological  
15 replicate for each genotype using bedtools intersect (55). The read coverage for the  
16 WT high confidence peaks was determined using bedtools coverage for all  
17 genotypes. To identify peaks with differential coverage, we used EdgeR to compare  
18 the WT peak coverage files to the corresponding mutant peak coverage; differential  
19 peaks were defined as having an FDR < 0.1 (56). To determine GTF2I high  
20 confidence peaks, we used peaks that had overlap between all four biological  
21 replicates and WT peaks with an FDR < 0.1 and log<sub>2</sub>FC > 0 when compared to the  
22 *Gtf2i*<sup>-/-</sup>/*Gtf2ird1*<sup>-/-</sup> IP coverage, since this mutation represents a full knockout of the  
23 protein.

1 Annotations of peaks and motif analysis was performed using the HOMER  
2 software on the high confidence peaks (57). Peaks were annotated at the  
3 transcription start (TSS) of genes if the peak overlapped the +2.5kbp or -1kbp of the  
4 TSS using a custom R script. GO analysis on the ChIP target genes was performed  
5 using the goseq R package. Comparison to ASD genes entailed testing for overlap  
6 between ChIP target genes and the genes identified by (28), their table S4, using  
7 Fisher's exact test and assuming 22,007 protein coding genes in the genome based  
8 on current NCBI annotation. Slightly more significant results were obtained when  
9 replicating this analysis using the SFARI gene database (58), accessed 8/4/2019,  
10 and testing for enrichment of score 1 and 2 ASD genes. We also analyzed pLI scores,  
11 downloaded from Gnomad (31) on 9/16/2019, of ChIP peaks. Similar results were  
12 obtained using pLI cutoffs of .9 and .99. For epigenetic overlaps, we used E13.5  
13 H3K4me3 and E13.5 H3K27me3 forebrain narrow bed peak files from the mouse  
14 ENCODE project to overlap with our peak datasets (59). Deeptools was used to  
15 generate bigwig files normalized to the library size for each sample by splitting the  
16 genome into 50bp overlapping bins (60). Deeptools was used to visualize the ChIP-  
17 seq coverage within the H3K4me3 and H3K27me3 peak regions. The LICR TFBS  
18 E14.5 whole brain CTCF peak data set was downloaded from the UCSC genome  
19 browser and lifted over to mm10 coordinates. TAD analysis of E14.5 cortical  
20 neuron HiC data (61) was carried out using domains previously called by arrowhead  
21 (Rao et al. Cell 2014, Clemens et al. *Mol Cell* in press). Domain boundaries were  
22 defined as 10kb regions centered on the start and end of each domain and lifted  
23 over to mm10 coordinates. Overlaps between GTF2IRD1 and GTF2I peaks and

1 other peak datasets was performed using the bedtools fisher function. PhyloP scores  
2 for the region underneath the WT ChIP-seq peaks and random genomic regions of  
3 the same length were retrieved using the UCSC table browser 60 Vertebrate  
4 Conservation PhyloP table. The Epigenome browser was used to visualize the ChIP-  
5 seq data as tracks (62).

6

7

8 *RNA-seq*

9

10 One microgram of E13.5 whole brain total RNA extracted from TRIzol LS was used  
11 as input for rRNA depletion using the NEBNext rRNA Depletion Kit  
12 (Human/Mouse/Rat). The rRNA-depleted RNA was used as input for library  
13 construction using the NEBNext Ultra II RNA library prep kit for Illumina. The final  
14 libraries were indexed and enriched by PCR using the following thermocycler  
15 conditions: 1) 98°C for 30 seconds, 2) 98°C 10 seconds, 3) 65°C 75 seconds, 4) 65°C  
16 5 minutes, 5) hold at 4°C, repeating steps 2-3 six times. The libraries were  
17 sequenced by the Genome Technology Access Center at Washington University  
18 School of Medicine on a HiSeq3000 producing 1x50 reads.

19

20 *RNA-seq analysis*

21

22 The raw RNA-seq reads were trimmed of Illumina adapters and bases with quality  
23 scores less than 25 using Trimmomatic Software. The trimmed reads were aligned

1 to the mm10 mouse genome using the default parameters of STARv2.6.1b (63). We  
2 used HTSeq-count to determine the read counts for features using the Ensembl  
3 GRCh38 version 93 gtf file (64). Differential gene expression analysis was done  
4 using EdgeR. We compared the expression of genes that are targets of either  
5 GTF2IRD1 or GTF2I to non-bound genes by generating a cumulative distribution  
6 plot of the average log CPM of the genes between genotypes. GO analysis was  
7 performed using the goseq R package.

8

#### 9 *Data Availability*

10

11 All RNA-seq and ChIP-seq data is available at GEO accession GSE138234.

12

13

#### 14 *Behavioral tasks*

15

16 All animal testing was done with approval from the Washington University in St.  
17 Louis Institutional Animal Care and Use Committee. Mice were group housed in  
18 same-sex, mixed-genotype cages with two to five mice per cage in standard mouse  
19 cages (dimensions 28.5 x 17.5 x 12 cm) on corn cob bedding. Mice had ad libitum  
20 access to food and water and followed a 12-hour light-dark cycle (light from  
21 6:00am-6:00pm). Animal housing rooms were kept at 20-22°C with a relative  
22 humidity of 50%. All mice were maintained on the FVB/AntJ (65) background from  
23 Jackson Labs. All behaviors were done in adulthood between ages P58-P133. A week



1 prior to behavioral testing mice were handled by the experimenter for habituation.  
2 On testing days the mice were moved to habituate to the testing room and the  
3 experimenter if male for 30 minutes before testing started.

4

## 5 **Ledge**

6

7 To test balance, we measured how long a mouse could balance on an acrylic ledge  
8 with a width of 0.5cm and a height of 38cm as described (65). The time when the  
9 mouse fell off the ledge was recorded up to 60 seconds when the trial was stopped.  
10 If the mouse fell off within five seconds, the time was restarted and the mouse  
11 received another attempt. If the mouse fell off within the first five seconds on the  
12 third attempt, that time was recorded. We tested all mice on the ledge twice, with a  
13 rest period of at least 20 minutes between trials. Trial average was used for analysis.

14

## 15 **One-hour locomotor activity**

16

17 We assessed activity levels in a one-hour locomotor task, as previously described  
18 (65). Mice were placed in the center of a standard rat-sized cage (dimensions 47.6 x  
19 25.4 x 20.6cm). The rat-sized cage was located inside a sound-attenuating box with  
20 white light at 24 lux. The mice could freely explore the cage for one hour. An acrylic  
21 lid with air holes was placed on top of the cage to prevent mice from jumping out.  
22 The position and horizontal movement of the mice was tracked using ANY-maze  
23 software (Stoelting Co., Wood dale, IL: RRID: SCR\_014289). The apparatus was

1 divided into two zones: a 33 x 11cm center zone and an edge zone of 5.5cm that  
2 bordered the cage. The animal was considered in a zone if 80% of the mouse was  
3 detected in that zone. ANY-maze recorded the time, distance, and number of entries  
4 into each zone. After the task, the mouse was returned to its home cage and the  
5 apparatus was thoroughly cleaned with 70% ethanol.

6

### 7 **Marble burying**

8

9 Marble burying is a species-specific task that measures the compulsive digging  
10 behavior of mice. Normal hippocampal function is thought to be required for normal  
11 phenotypes in this task. We tested marble burying as described previously (65). A  
12 rat cage was filled with aspen bedding to a depth of 3cm and placed in a sound-  
13 attenuating box with white light set to 24 lux. Twenty marbles were placed on top of  
14 the bedding in a 5 x 4 evenly spaced grid. The experimental mouse was placed in the  
15 center of the chamber and allowed to freely explore and dig for 30 minutes. An  
16 acrylic lid with air holes was placed on top of the cage to prevent mice from  
17 escaping. After 30 minutes, the animal was returned to its home cage. Two scorers  
18 counted the number of marbles not buried (less than two-thirds of the marble was  
19 covered with bedding). The number of marbles buried was then determined, and  
20 the average of the two scores was used in the analysis. After the marbles were  
21 counted, the bedding was disposed of and the cage and marbles were cleaned with  
22 70% ethanol.

23

## 1 **Pre-pulse inhibition**

2

3 Pre-pulse inhibition (PPI) measures the suppression of the acoustic startle reflex  
4 when an animal is presented with a smaller stimulus (pre-pulse) before a more  
5 intense stimulus (startle). Acoustic startle response and pre-pulse inhibition were  
6 measured as previously described (23). Startle Monitor II software was used to run  
7 the protocol in a sound-attenuating chamber (Kinder Scientific, LLC, Poway, CA).  
8 Mice were secured in a small enclosure and placed on a force-sensitive plate inside  
9 the chamber. Animals were acclimated to the test chamber for 5 minutes before  
10 trials began. Startle amplitude was recorded with 1ms force readings during 65  
11 pseudo-randomized trials that alternated between various stimulus conditions. An  
12 auditory stimulus of 120dB was presented for 40ms to illicit the startle response.  
13 Pre-pulse inhibition was measured in three different types of trials where the  
14 120dB stimulus was preceded by pre-pulses of 4, 8, and 16 dB above the  
15 background sound level (65dB). PPI was calculated by using the average startle  
16 response (measured in Newtons) of the 120dB stimulus trials minus the average  
17 startle response to the stimulus after each respective pre-pulse level. This was  
18 divided by the 120dB stimulus startle response and multiplied by 100 to get a  
19 percent inhibition of startle.

20

## 21 **Contextual and Cued Fear Conditioning**

22

1 Learning and memory were tested using the contextual and cued fear conditioning  
2 paradigm as previously described (66). Contextual fear memory is thought to be  
3 driven by hippocampal functioning whereas cued fear is thought to be driven by  
4 amygdala functioning. On day one of the experiment, animals were placed in an  
5 acrylic chamber (26cm x 18cm x 18cm; Med Associates Inc., Fairfax, VT) with a  
6 metal grid floor and a peppermint odor from an unobtainable source. The chamber  
7 light was on for the duration of the five-minute task. During the first two minutes,  
8 the animal freely explored the apparatus to measure baseline freezing. At 100  
9 seconds, 160 seconds, and 220 seconds, an 80dB white noise tone (conditioned  
10 stimulus, CS) was played for a duration of 20 seconds. During the last two seconds of  
11 this tone, the mice received a 1.0mA foot shock (unconditioned stimulus, UCS). The  
12 animal's freezing behavior was monitored by FreezeFrame software (Actimetrics,  
13 Evanston, IL) in 0.75s intervals. Freezing was defined as no movement besides  
14 respiration and was used as a measure of the fear response in mice. After the five-  
15 minute task, the mice were returned to their home cage. On day two, we tested  
16 contextual fear memory. The mice were placed in the same chamber as day one with  
17 the peppermint odor, and freezing behavior was measured over eight minutes. The  
18 first two minutes of day two were compared to the first two minutes of day one to  
19 test for the acquisition of fear memory. The mice were then returned to their home  
20 cage. On day three, to test cued fear, the mice were placed in a new black and white  
21 chamber that was partitioned into a triangle shape and had a new coconut scent.  
22 The mice were allowed to explore the chamber and the first two minutes were  
23 considered baseline. After minute two the 80dB tone (CS) was played for the

1 remaining eight minutes. Freezing behavior was monitored during the entire ten-  
2 minute task.

3

#### 4 **Shock sensitivity**

5

6 We tested the shock sensitivity of the mice to ensure that differences in conditioned  
7 fear were not due to differing responses to the shock itself, following a previously  
8 established protocol (23). Mice were placed in the apparatus used for day one and  
9 day two of the conditioned fear task. The mice were delivered a two second 0.05mA  
10 shock and their behavior was observed. The shock was increased by 0.05mA up to  
11 1mA or until the mice exhibited flinching, escape, and vocalization behaviors. Once  
12 the mouse had shown each behavior, the test was ended and the final mA used was  
13 recorded.

14

#### 15 *Statistical Analysis*

16

17 All statistical analyses were performed in R v3.4.2 and are reported in Supplemental  
18 Table 3. The ANOVA assumption of normality was assessed using the Shapiro-  
19 Wilkes test and manual inspection of qqPlots, and the assumption of equal variances  
20 was assessed with Levene's Test. When appropriate, ANOVA was used to test for  
21 main effects and interaction terms. Post hoc analyses were done to compare  
22 between genotypes. If the data violated the assumptions of ANOVA, non-parametric  
23 tests were performed. If the experiment was performed over time, linear mixed

1 models were used to account for the repeated measures of an animal using the lme4  
2 R package. Post hoc analyses were then conducted to compare between genotypes  
3 within time bins. Post hoc analyses were done using the multcomp R package (67).  
4 Animals were removed from analysis if they had a value that was 3.29 standard  
5 deviations above the mean or had poor video tracking and could not be analyzed.

6

### 7 **Acknowledgements**

8 This work was supported by 1R01MH107515 JDD, and the Autism Science Foundation, and  
9 the National Science Foundation Graduate Research Fellowship DGE-1745038 to NDK and  
10 DGE-1745038 to KRN. We would like to thank the Genome Technology Access Center for  
11 technical support, as well as Dr. Beth Kozel for critical advice on this project. We would also  
12 like to thank Dr. David Wozniak and the Animal Behavior Core at the Washington University  
13 School of Medicine for their support.

14

### 15 **Conflict of Interest Statement**

16 None of the authors have any conflict of interest that could bias the work presented here.

17

### 18 **References**

19

- 20 1. Merla, G., Brunetti-Pierri, N., Micale, L., et al. (2010) Copy number variants at  
21 Williams–Beuren syndrome 7q11.23 region. *Hum Genet*, **128**, 3–26.
- 22 2. Meyer-Lindenberg, A., Mervis, C. B. and Faith Berman, K. (2006) Neural  
23 mechanisms in Williams syndrome: a unique window to genetic influences  
24 on cognition and behaviour. *Nat Rev Neurosci*, **7**, 380–393.
- 25 3. Korenberg, J. R., Chen, X.-N., Hirota, H., et al. (2000) VI. Genome Structure and  
26 Cognitive Map of Williams Syndrome. *Journal of Cognitive Neuroscience*, **12**,  
27 89–107.
- 28 4. Sakurai, T., Dorr, N. P., Takahashi, N., et al. (2011) Haploinsufficiency of Gtf2i,  
29 a gene deleted in Williams Syndrome, leads to increases in social  
30 interactions. *Autism Res*, **4**, 28–39.
- 31 5. Segura-Puimedon, M., Sahún, I., Velot, E., et al. (2014) Heterozygous deletion  
32 of the Williams–Beuren syndrome critical interval in mice recapitulates most  
33 features of the human disorder. *Hum. Mol. Genet.*, **23**, 6481–6494.
- 34 6. Li, H. H., Roy, M., Kuscuoglu, U., et al. (2009) Induced chromosome deletions  
35 cause hypersociability and other features of Williams–Beuren syndrome in  
36 mice. *EMBO Molecular Medicine*, **1**, 50–65.

- 1 7. Osborne, L. R. (2010) Animal models of Williams syndrome. *Am. J. Med. Genet.*, **154C**, 209–219.
- 3 8. Young, E. J., Lipina, T., Tam, E., et al. (2008) Reduced fear and aggression and altered serotonin metabolism in Gtf2ird1-targeted mice. *Genes, Brain and Behavior*, **7**, 224–234.
- 6 9. Howard, M. L., Palmer, S. J., Taylor, K. M., et al. (2012) Mutation of Gtf2ird1 from the Williams–Beuren syndrome critical region results in facial dysplasia, motor dysfunction, and altered vocalisations. *Neurobiology of Disease*, **45**, 913–922.
- 10 10. Schaefer, M. L., Wong, S. T., Wozniak, D. F., et al. (2000) Altered stress-induced anxiety in adenylyl cyclase type VIII-deficient mice. *J. Neurosci.*, **20**, 4809–4820.
- 13 11. Barak, B., Zhang, Z., Liu, Y., et al. (2019) Neuronal deletion of Gtf2i, associated with Williams syndrome, causes behavioral and myelin alterations rescuable by a remyelinating drug. *Nature Neuroscience*, **22**, 700.
- 16 12. Martin, L. A., Iceberg, E. and Allaf, G. (2018) Consistent hypersocial behavior in mice carrying a deletion of Gtf2i but no evidence of hyposocial behavior with Gtf2i duplication: Implications for Williams-Beuren syndrome and autism spectrum disorder. *Brain Behav*, **8**, e00895.
- 20 13. Porter, M. A., Dobson-Stone, C., Kwok, J. B. J., et al. (2012) A Role for Transcription Factor GTF2IRD2 in Executive Function in Williams-Beuren Syndrome. *PLOS ONE*, **7**, e47457.
- 23 14. Gunbin, K. V. and Ruvinsky, A. (2012) Evolution of General Transcription Factors. *J Mol Evol*, **76**, 28–47.
- 25 15. Bayarsaihan, D. and Ruddle, F. H. (2000) Isolation and characterization of BEN, a member of the TFII-I family of DNA-binding proteins containing distinct helix–loop–helix domains. *PNAS*, **97**, 7342–7347.
- 28 16. Cheriya, V., Desgranges, Z. P. and Roy, A. L. (2002) c-Src-dependent Transcriptional Activation of TFII-I. *J. Biol. Chem.*, **277**, 22798–22805.
- 30 17. Caraveo, G., Rossum, D. B. van, Patterson, R. L., et al. (2006) Action of TFII-I Outside the Nucleus as an Inhibitor of Agonist-Induced Calcium Entry. *Science*, **314**, 122–125.
- 33 18. Carmona-Mora, P., Widagdo, J., Tomasetig, F., et al. (2015) The nuclear localization pattern and interaction partners of GTF2IRD1 demonstrate a role in chromatin regulation. *Hum Genet*, **134**, 1099–1115.

- 1 19. Makeyev, A. V., Enkhmandakh, B., Hong, S.-H., et al. (2012) Diversity and  
2 Complexity in Chromatin Recognition by TFII-I Transcription Factors in  
3 Pluripotent Embryonic Stem Cells and Embryonic Tissues. *PLOS ONE*, **7**,  
4 e44443.
- 5 20. Bayarsaihan, D., Makeyev, A. V. and Enkhmandakh, B. (2012) Epigenetic  
6 modulation by TFII-I during embryonic stem cell differentiation. *Journal of*  
7 *Cellular Biochemistry*, **113**, 3056–3060.
- 8 21. Schneider, T., Skitt, Z., Liu, Y., et al. (2012) Anxious, hypoactive phenotype  
9 combined with motor deficits in Gtf2ird1 null mouse model relevant to  
10 Williams syndrome. *Behavioural Brain Research*, **233**, 458–473.
- 11 22. Dai, L., Bellugi, U., Chen, X.-N., et al. (2009) Is it Williams syndrome?  
12 GTF2IRD1 implicated in visual–spatial construction and GTF2I in sociability  
13 revealed by high resolution arrays. *Am. J. Med. Genet.*, **149A**, 302–314.
- 14 23. Kopp, N., McCullough, K., Maloney, S. E., et al. (2019) Gtf2i and Gtf2ird1  
15 mutation do not account for the full phenotypic effect of the Williams  
16 syndrome critical region in mouse models. *Hum Mol Genet.*
- 17 24. Lazebnik, M. B., Tussie-Luna, M. I. and Roy, A. L. (2008) Determination and  
18 Functional Analysis of the Consensus Binding Site for TFII-I Family Member  
19 BEN, Implicated in Williams-Beuren Syndrome. *J. Biol. Chem.*, **283**, 11078–  
20 11082.
- 21 25. Peña-Hernández, R., Marques, M., Hilmi, K., et al. (2015) Genome-wide  
22 targeting of the epigenetic regulatory protein CTCF to gene promoters by the  
23 transcription factor TFII-I. *PNAS*, **112**, E677–E686.
- 24 26. Yue, F., Cheng, Y., Breschi, A., et al. (2014) A comparative encyclopedia of  
25 DNA elements in the mouse genome. *Nature*, **515**, 355–364.
- 26 27. Sanders, S. J., Ercan-Sencicek, A. G., Hus, V., et al. (2011) Multiple recurrent de  
27 novo CNVs, including duplications of the 7q11.23 Williams syndrome region,  
28 are strongly associated with autism. *Neuron*, **70**, 863–885.
- 29 28. Satterstrom, F. K., Kosmicki, J. A., Wang, J., et al. (2018) Novel genes for  
30 autism implicate both excitatory and inhibitory cell lineages in risk. *bioRxiv*,  
31 484113.
- 32 29. Kopp, N., Climer, S. and Dougherty, J. D. (2015) Moving from capstones  
33 toward cornerstones: successes and challenges in applying systems biology  
34 to identify mechanisms of autism spectrum disorders. *Front Genet*, **6**.



- 1 30. Parikshak, N. N., Luo, R., Zhang, A., et al. (2013) Integrative Functional  
2 Genomic Analyses Implicate Specific Molecular Pathways and Circuits in  
3 Autism. *Cell*, **155**, 1008–1021.
- 4 31. Karczewski, K. J., Francioli, L. C., Tiao, G., et al. (2019) Variation across  
5 141,456 human exomes and genomes reveals the spectrum of loss-of-  
6 function intolerance across human protein-coding genes. *bioRxiv*, 531210.
- 7 32. Palmer, S. J., Santucci, N., Widagdo, J., et al. (2010) Negative Autoregulation of  
8 GTF2IRD1 in Williams-Beuren Syndrome via a Novel DNA Binding  
9 Mechanism. *J. Biol. Chem.*, **285**, 4715–4724.
- 10 33. Hinsley, T. A., Cunliffe, P., Tipney, H. J., et al. (2004) Comparison of TFII-I gene  
11 family members deleted in Williams-Beuren syndrome. *Protein Science*, **13**,  
12 2588–2599.
- 13 34. O’Leary, J. and Osborne, L. R. (2011) Global Analysis of Gene Expression in  
14 the Developing Brain of Gtf2ird1 Knockout Mice. *PLoS ONE*, **6**, e23868.
- 15 35. Tassabehji, M., Hammond, P., Karmiloff-Smith, A., et al. (2005) GTF2IRD1 in  
16 Craniofacial Development of Humans and Mice. *Science*, **310**, 1184–1187.
- 17 36. Borralleras, C., Sahun, I., Pérez-Jurado, L. A., et al. (2015) Intracisternal Gtf2i  
18 Gene Therapy Ameliorates Deficits in Cognition and Synaptic Plasticity of a  
19 Mouse Model of Williams–Beuren Syndrome. *Mol Ther.*
- 20 37. Dykens, E. M. (2003) Anxiety, Fears, and Phobias in Persons With Williams  
21 Syndrome. *Developmental Neuropsychology*, **23**, 291–316.
- 22 38. Enkhmandakh, B., Makeyev, A. V., Erdenechimeg, L., et al. (2009) Essential  
23 functions of the Williams-Beuren syndrome-associated TFII-I genes in  
24 embryonic development. *PNAS*, **106**, 181–186.
- 25 39. Widagdo, J., Taylor, K. M., Gunning, P. W., et al. (2012) SUMOylation of  
26 GTF2IRD1 Regulates Protein Partner Interactions and Ubiquitin-Mediated  
27 Degradation. *PLoS ONE*, **7**, e49283.
- 28 40. Sinai, L., Ivakine, E. A., Lam, E., et al. (2015) Disruption of Src Is Associated  
29 with Phenotypes Related to Williams-Beuren Syndrome and Altered Cellular  
30 Localization of TFII-I. *eNeuro*, **2**, ENEURO.0016-14.2015.
- 31 41. Wade, A. A., Lim, K., Catta-Preta, R., et al. (2019) Common CHD8 Genomic  
32 Targets Contrast With Model-Specific Transcriptional Impacts of CHD8  
33 Haploinsufficiency. *Front. Mol. Neurosci.*, **11**.

- 1 42. Tudor, M., Akbarian, S., Chen, R. Z., et al. (2002) Transcriptional profiling of a  
2 mouse model for Rett syndrome reveals subtle transcriptional changes in the  
3 brain. *PNAS*, **99**, 15536–15541.
- 4 43. Chahrour, M., Jung, S. Y., Shaw, C., et al. (2008) MeCP2, a key contributor to  
5 neurological disease, activates and represses transcription. *Science*, **320**,  
6 1224–1229.
- 7 44. Stroud, H., Su, S. C., Hrvatin, S., et al. (2017) Early-Life Gene Expression in  
8 Neurons Modulates Lasting Epigenetic States. *Cell*, **171**, 1151-1164.e16.
- 9 45. Fazel Darbandi, S., Robinson Schwartz, S. E., Qi, Q., et al. (2018) Neonatal  
10 Tbr1 Dosage Controls Cortical Layer 6 Connectivity. *Neuron*, **100**, 831-  
11 845.e7.
- 12 46. Guy, J., Hendrich, B., Holmes, M., et al. (2001) A mouse *Mecp2* -null mutation  
13 causes neurological symptoms that mimic Rett syndrome. *Nature Genetics*,  
14 **27**, 322–326.
- 15 47. Lucena, J., Pezzi, S., Aso, E., et al. (2010) Essential role of the N-terminal  
16 region of TFII-I in viability and behavior. *BMC Medical Genetics*, **11**, 61.
- 17 48. Deacon, R. M. J., Croucher, A. and Rawlins, J. N. P. (2002) Hippocampal  
18 cytotoxic lesion effects on species-typical behaviours in mice. *Behavioural*  
19 *Brain Research*, **132**, 203–213.
- 20 49. van Hagen, J. M., van der Geest, J. N., van der Giessen, R. S., et al. (2007)  
21 Contribution of CYLN2 and GTF2IRD1 to neurological and cognitive  
22 symptoms in Williams Syndrome. *Neurobiology of Disease*, **26**, 112–124.
- 23 50. Botta, A., Novelli, G., Mari, A., et al. (1999) Detection of an atypical 7q11.23  
24 deletion in Williams syndrome patients which does not include the STX1A  
25 and FZD3 genes. *Journal of Medical Genetics*, **36**, 478–480.
- 26 51. Grueneberg, D. A., Henry, R. W., Brauer, A., et al. (1997) A multifunctional  
27 DNA-binding protein that promotes the formation of serum response  
28 factor/homeodomain complexes: identity to TFII-I. *Genes Dev.*, **11**, 2482–  
29 2493.
- 30 52. Bolger, A. M., Lohse, M. and Usadel, B. (2014) Trimmomatic: a flexible  
31 trimmer for Illumina sequence data. *Bioinformatics*, **30**, 2114–2120.
- 32 53. Langmead, B., Wilks, C., Antonescu, V., et al. (2019) Scaling read aligners to  
33 hundreds of threads on general-purpose processors. *Bioinformatics*, **35**, 421–  
34 432.

- 1 54. Zhang, Y., Liu, T., Meyer, C. A., et al. (2008) Model-based Analysis of ChIP-Seq  
2 (MACS). *Genome Biology*, **9**, R137.
- 3 55. Quinlan, A. R. and Hall, I. M. (2010) BEDTools: a flexible suite of utilities for  
4 comparing genomic features. *Bioinformatics*, **26**, 841–842.
- 5 56. Robinson, M. D., McCarthy, D. J. and Smyth, G. K. (2010) edgeR: a  
6 Bioconductor package for differential expression analysis of digital gene  
7 expression data. *Bioinformatics*, **26**, 139–140.
- 8 57. Heinz, S., Benner, C., Spann, N., et al. (2010) Simple Combinations of Lineage-  
9 Determining Transcription Factors Prime cis-Regulatory Elements Required  
10 for Macrophage and B Cell Identities. *Molecular Cell*, **38**, 576–589.
- 11 58. Abrahams, B. S., Arking, D. E., Campbell, D. B., et al. (2013) SFARI Gene 2.0: a  
12 community-driven knowledgebase for the autism spectrum disorders  
13 (ASDs). *Mol Autism*, **4**, 36.
- 14 59. Stamatoyannopoulos, J. A., Snyder, M., Hardison, R., et al. (2012) An  
15 encyclopedia of mouse DNA elements (Mouse ENCODE). *Genome Biology*, **13**,  
16 418.
- 17 60. Ramírez, F., Ryan, D. P., Grüning, B., et al. (2016) deepTools2: a next  
18 generation web server for deep-sequencing data analysis. *Nucleic Acids Res*,  
19 **44**, W160–W165.
- 20 61. Bonev, B., Cohen, N. M., Szabo, Q., et al. (2017) Multiscale 3D Genome  
21 Rewiring during Mouse Neural Development. *Cell*, **171**, 557–572.e24.
- 22 62. Li, D., Hsu, S., Purushotham, D., et al. (2019) WashU Epigenome Browser  
23 update 2019. *Nucleic Acids Res*, **47**, W158–W165.
- 24 63. Dobin, A., Davis, C. A., Schlesinger, F., et al. (2013) STAR: ultrafast universal  
25 RNA-seq aligner. *Bioinformatics*, **29**, 15–21.
- 26 64. Anders, S., Pyl, P. T. and Huber, W. (2015) HTSeq—a Python framework to  
27 work with high-throughput sequencing data. *Bioinformatics*, **31**, 166–169.
- 28 65. Maloney, S. E., Akula, S., Rieger, M. A., et al. (2018) Examining the  
29 Reversibility of Long-Term Behavioral Disruptions in Progeny of Maternal  
30 SSRI Exposure. *eNeuro*, **5**.
- 31 66. Maloney, S. E., Yuede, C. M., Creeley, C. E., et al. (2019) Repeated neonatal  
32 isoflurane exposures in the mouse induce apoptotic degenerative changes in  
33 the brain and relatively mild long-term behavioral deficits. *Scientific Reports*,  
34 **9**, 2779.

1 67. Hothorn, T., Bretz, F. and Westfall, P. (2008) Simultaneous Inference in  
 2 General Parametric Models. *Biometrical Journal*, **50**, 346–363.

3  
 4  
 5  
 6  
 7  
 8  
 9

**Table 1: Behaviors and sample sizes for *Gtf2ird1*<sup>+/-</sup> x *Gtf2ird1*<sup>+/-</sup> cross**

Cohort		male			female		
Behavior	Experimenter	WT	<i>Gtf2ird1</i> <sup>+/-</sup>	<i>Gtf2ird1</i> <sup>-/-</sup>	WT	<i>Gtf2ird1</i> <sup>+/-</sup>	<i>Gtf2ird1</i> <sup>-/-</sup>
1-hour locomotor activity	Female	10	21	12	15	16	17
Ledge	Female	9	21	13	15	17	17
Marble burying	Female	8	20	10	14	17	14
Pre-pulse inhibition	Female	8	20	11	14	17	15
Conditioned fear	Female	9	18	10	15	17	17
Shock sensitivity	Female	9	10	11	15	17	17

10  
 11  
 12  
 13

**Table 2: Behaviors and sample sizes for *Gtf2ird1*<sup>+/-</sup> x *Gtf2i*<sup>+/-</sup>/*Gtf2ird1*<sup>+/-</sup> cross**

Cohort1		male				female			
Behavior	Experimenter	WT	<i>Gtf2ird1</i> <sup>+/-</sup>	<i>Gtf2i</i> <sup>+/-</sup> / <i>Gtf2ird1</i> <sup>+/-</sup>	<i>Gtf2i</i> <sup>+/-</sup> / <i>Gtf2ird1</i> <sup>-/-</sup>	WT	<i>Gtf2ird1</i> <sup>+/-</sup>	<i>Gtf2i</i> <sup>+/-</sup> / <i>Gtf2ird1</i> <sup>+/-</sup>	<i>Gtf2i</i> <sup>+/-</sup> / <i>Gtf2ird1</i> <sup>-/-</sup>
1-hour locomotor activity	Male	8	8	11	7	14	9	9	11
Ledge	Male	8	8	12	7	14	9	11	11
Marble burying	Male	8	8	12	7	14	9	11	11
<b>Cohort2</b>									
Pre-pulse inhibition	Male	13	6	12	6	11	15	13	12
Conditioned fear	Male	11	4	9	5	7	13	12	11
Shock sensitivity	Male	12	6	10	6	10	15	13	12

14  
 15  
 16  
 17

## Figure Legends

18 **Figure 1: GTF2IRD1 binds preferentially to promoters in conserved, active**  
 19 **sites in the genome. A** GTF2IRD1 binding peaks are annotated primarily in  
 20 promoters and gene bodies. The distribution of peak annotations is significantly  
 21 different from random sampling of the genome. **B** GTF2IRD1 peaks were enriched in  
 22 H3K4me3 sites marking active regions of the genome and to a lesser extent in

1 H3K27me3 sites marking repressed regions. **C** GO analysis of genes that have  
2 GTF2IRD1 bound to the promoter. **D** The conservation of sequence in GTF2IRD1-  
3 bound peaks is significantly higher than expected by chance. **E** Motifs of  
4 transcription factors enriched under Gtf2ird1 bound peaks.

5

6 **Figure 2: GTF2I binds at promoters in conserved, active sites in the genome. A**

7 GTF2I binding sites are annotated mostly in gene promoters and the gene body. The  
8 distribution of peaks is significantly different than would be expected by chance. **B**  
9 GTF2I peaks overlap with H3K4me3 peaks marking active regions and to a lesser  
10 extent GTF2I peaks fall within H3K27me3 peaks marking inactive regions. **C** GO  
11 analysis of genes that have GTF2I bound at the promoter. **D** Epigenome browser  
12 shot of GTF2I peak bound within the *Src* gene. **E** Genomic sequence under GTF2I  
13 peaks are more conserved than we would expect by chance. **F** Motifs of  
14 transcription factors that are enriched in GTF2I bound sequences.

15

16 **Figure 3: Comparison of GTF2IRD1 and GTF2I binding sites. A** GTF2I and

17 GTF2IRD1 have different distributions of annotated binding sites. **B** GTF2IRD1  
18 bound sequences are more conserved than GTF2I bound sequences. **C** The overlap  
19 of genes that have GTF2I and GTF2IRD1 bound at their promoters. **D** Motifs of  
20 transcription factors that are enriched in regions bound by both GTF2I and  
21 GTF2IRD1. **E** GO analysis of genes with both GTF2I and GTF2IRD1 bound at their  
22 promoters. **F** Epigenome browser shot of *Mapk14* showing peaks for both GTF2I and

1 GTF2IRD1. **G** Enrichment of GTF2IRD1 and GTF2I bound genes in ASD and  
2 conserved gene sets.  
3  
4 **Figure 4: Frameshift mutation in *Gtf2ird1* exon three results in a decreased**  
5 **amount of an N-truncated protein with diminished binding at *Gtf2ird1***  
6 **promoter and has little effect on transcription in the brain. **A**** The sequence of  
7 exon three of *Gtf2ird1* targeted by the underlined gRNA with the PAM sequence in  
8 blue. The mutant allele contains a one base pair insertion of an adenine nucleotide  
9 that results in a premature stop codon. **B** Breeding scheme of the intercross of  
10 *Gtf2ird1*<sup>+/-</sup> to produce genotypes used in the experiments. **C, D** Mutation in *Gtf2ird1*  
11 does not affect the protein or transcript levels of *Gtf2i*. **E** Frameshift mutation  
12 decreases the amount of protein in *Gtf2ird1*<sup>-/-</sup> and causes a slight shift to lower  
13 molecular weight. **F** The abundance of *Gtf2ird1* transcript increases with increasing  
14 dose of the mutation. **G** Schematic of *Gtf2ird1* upstream regulatory element (GUR)  
15 that shows the three GTF2IRD1 binding motifs. The arrows indicate the location of  
16 the primers for amplifying the GUR in the ChIP-qPCR assay. **H,I** WT ChIP of  
17 GTF2IRD1 shows enrichment of the GUR over off target regions. There is more  
18 enrichment in the WT genotype compared to the *Gtf2ird1*<sup>-/-</sup> genotype. **J** Profile plots  
19 of GTF2IRD1 ChIP-seq data confirms diminished binding at the *Gtf2ird1* promoter. **K**  
20 Differential peak analysis comparing WT and *Gtf2ird1*<sup>-/-</sup> ChIP-seq data showed only  
21 the peak at *Gtf2ird1* is changed between genotypes with an FDR <0.1. **L** Differential  
22 expression analysis in the E13.5 brain comparing WT and *Gtf2ird1*<sup>-/-</sup> showed only  
23 *Gtf2ird1* as changed with FDR <0.1. **M** The presence of GTF2IRD1 at gene promoters

1 is not evenly distributed across expression levels. **N** The expression of genes bound  
2 by GTF2IRD1 is not different compared to all other genes between WT and *Gtf2ird1*  
3 *-/-* mutants.

4

5 **Figure 5: Homozygous frameshift mutation in *Gtf2ird1* is sufficient to cause**

6 **behavioral phenotypes. A** Homozygous mutants have worse balance than WT

7 littermates in ledge task. **B** Homozygous mutants bury fewer marbles than WT and

8 heterozygous littermates. **C** Overall activity levels are not affected but a time by

9 genotype interaction shows the mutant animals are slower to habituate to the novel

10 environment. **D** There is no difference in time spent in the center of the apparatus

11 between genotypes. **E** All animals show an increase in startle inhibition when given

12 a pre-pulse of increasing intensity. There is no difference between genotypes. **F**

13 Acquisition phase of fear conditioning paradigm. All animals show the expected

14 increase in freezing to additional foot shocks. **G** *Gtf2ird1*<sup>-/-</sup> animals show an early

15 increased contextual fear memory response compared to WT and heterozygous

16 littermates. **H** There were no significant differences between genotypes in cued fear.

17

18 **Figure 6: Mutating both *Gtf2i* and *Gtf2ird1* does not result in larger differences**

19 **in brain transcriptomes. A** Generation of double mutant. gRNA target is

20 underlined in exon five of *Gtf2i* with the PAM sequence in blue. The two base pair

21 deletion results in a premature stop codon within exon five. The *Gtf2ird1* mutation

22 is a large 590bp deletion covering most of exon three as shown in the IGV browser

23 shot. **B** Heterozygous intercross to generate genotypes for ChIP and RNA-seq

1 experiments. The homozygous double mutants are embryonic lethal but are present  
2 up to E15.5. **C** The two base pair deletion in *Gtf2i* decreases the protein by 50% in  
3 heterozygous mutants and no protein is detected in the homozygous E13.5 brain. **D**  
4 The mutation decreases the abundance of *Gtf2i* transcript consistent with nonsense-  
5 mediated decay. **E** The 590bp deletion in *Gtf2ird1* leads to decreased protein levels  
6 in heterozygous and homozygous mutants. There is still a small amount of protein  
7 made in the homozygous mutant. **F** The 590bp deletion increases the amount of  
8 *Gtf2ird1* transcript. **G** Volcano plot comparing the expression in the E13.5 brain of  
9 WT and heterozygous double mutants. The highlighted genes represent an FDR  
10 <0.1. **H** The presence of *Gtf2i* at the promoters does not correlate with the  
11 expression of a gene. **I** The fold change of genes between WT and heterozygous  
12 double mutants that have GTF2I bound at their promoters were slightly upregulated  
13 when compared to the fold change of genes that did not have GTF2I bound.

14

15 **Figure 7: *Gtf2i* does not modify most of the phenotypes of *Gtf2ird1* mutation. **A****  
16 **Breeding scheme for behavior experiments. **B** The *Gtf2i*<sup>+/-</sup>/*Gtf2ird1*<sup>-/-</sup> animals fell off**  
17 **ledge sooner than WT littermates. **C** There was a main effect of genotype on marbles**  
18 **buried. Post hoc analysis showed that *Gtf2i*<sup>+/-</sup>/*Gtf2ird1*<sup>-/-</sup> buried fewer marbles than**  
19 **the *Gtf2ird1*<sup>-/-</sup> genotype. **D** *Gtf2i*<sup>+/-</sup>/*Gtf2ird1*<sup>-/-</sup> had increased overall activity levels in**  
20 **a one-hour activity task. **E** *Gtf2i*<sup>+/-</sup>/*Gtf2ird1*<sup>-/-</sup> showed decreased time in the center of**  
21 **the apparatus compared to WT. **F** All animals show an increased startle inhibition**  
22 **when given a pre-pulse of increasing intensity. The double mutants show less of an**  
23 **inhibition at higher pre-pulse levels compared to WT and *Gtf2ird1*<sup>+/-</sup> animals. **G** All**



1 genotypes showed increased freezing with subsequent foot shocks. **H** All genotypes  
2 showed a similar contextual fear response. **I** There was a main effect of genotype on  
3 cued fear with the *Gtf2ird1*<sup>+/-</sup> and *Gtf2i*<sup>+/-</sup>/*Gtf2ird1*<sup>-/-</sup> genotypes showing an increased  
4 fear response compared to WT.

5

6

## Figure 1: GTF2IRD1 binds preferentially to promoters in conserved, active sites in the genome.

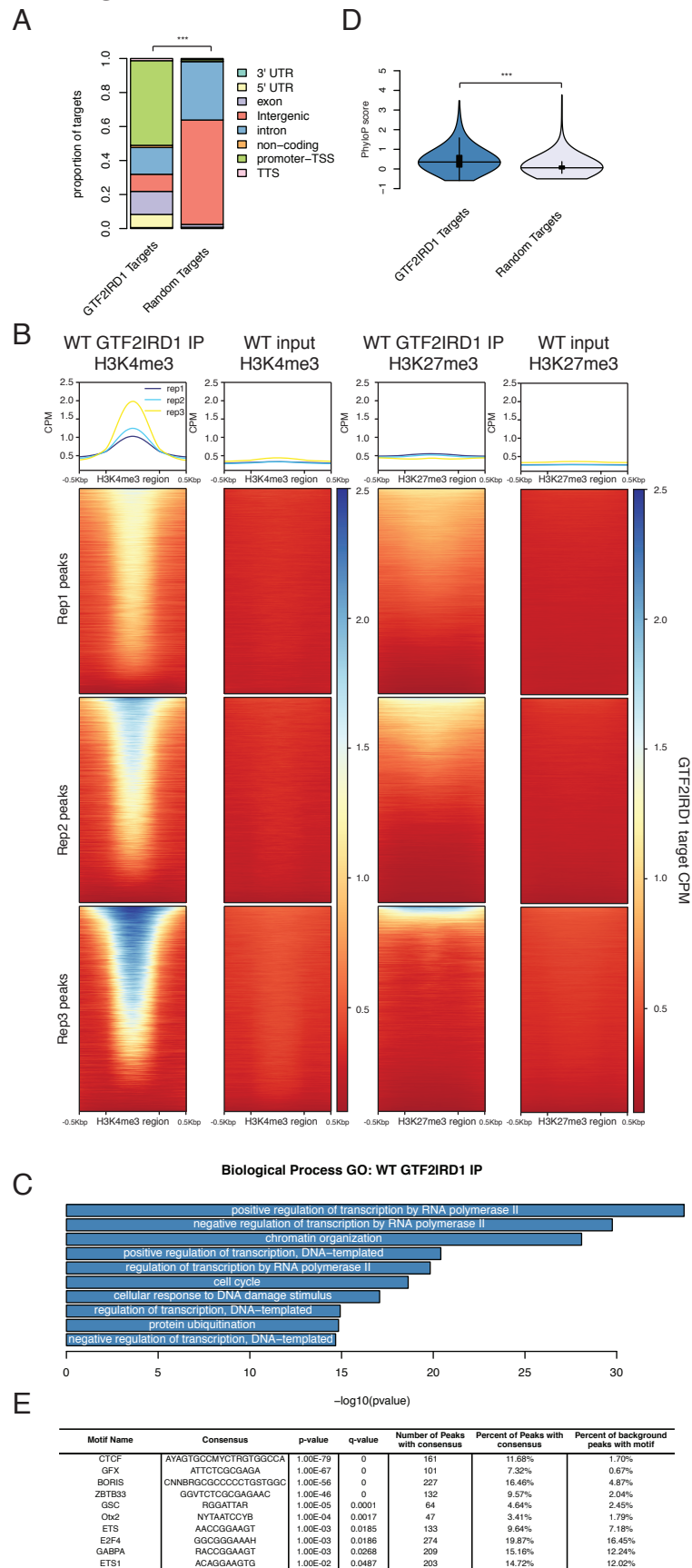


**Figure 2: GTF2I binds at promoters in conserved, active sites in the genome.**

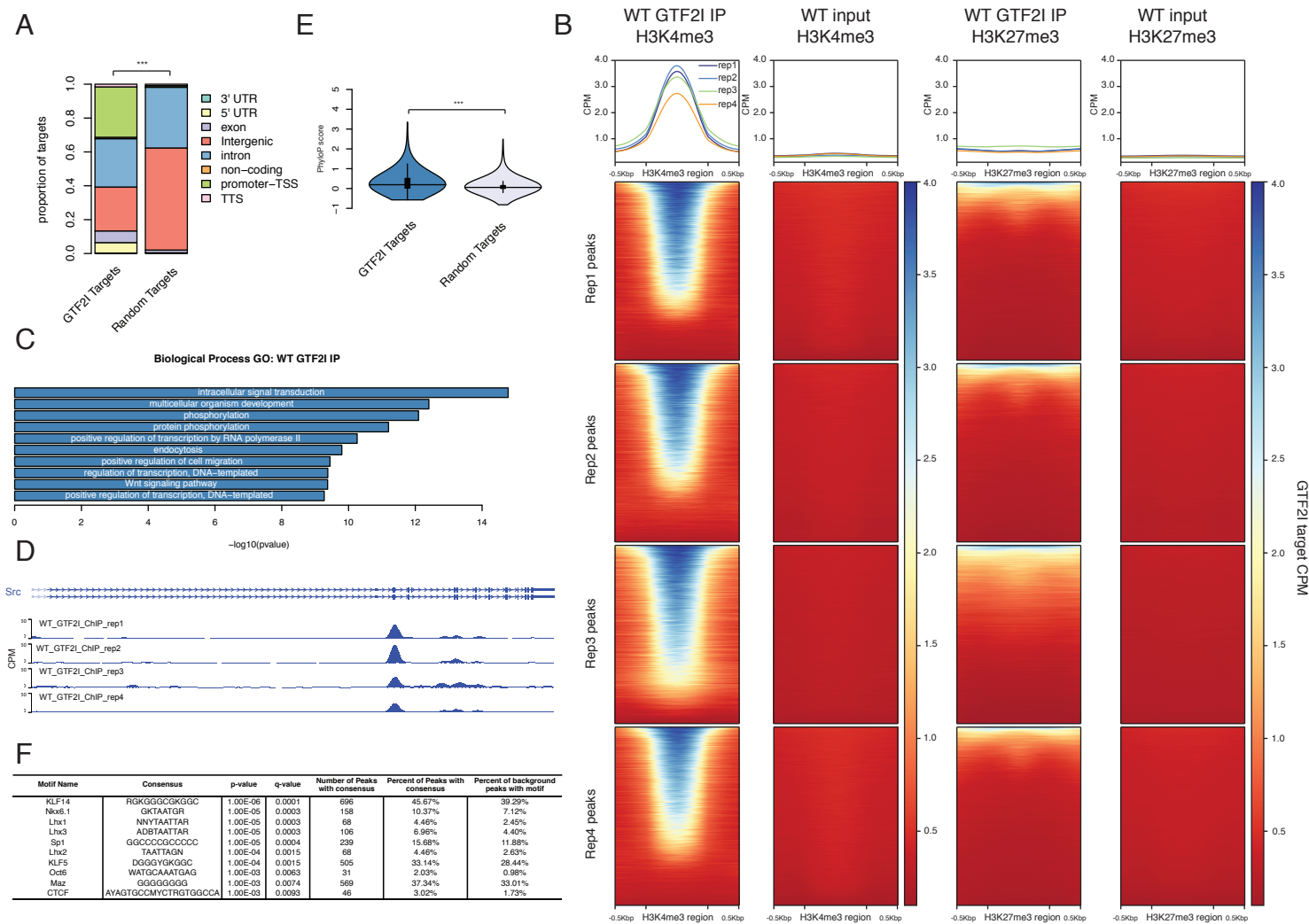


**Figure 3: Comparison of GTF2IRD1 and GTF2I binding sites.**

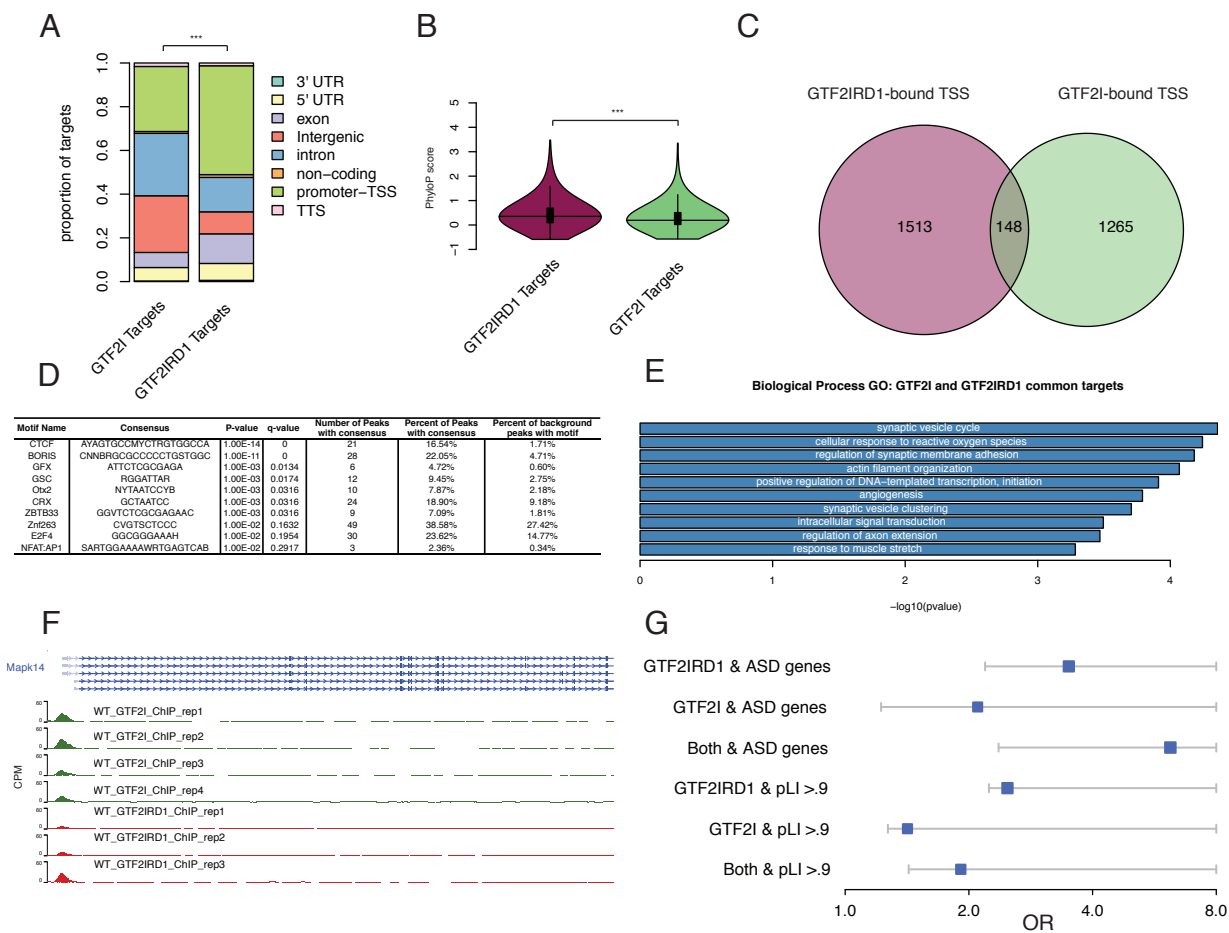


## Figure 4: Frameshift mutation in Gtf2ird1 exon three results in a decreased amount of an N-truncated protein with diminished binding at Gtf2ird1 promoter and has little effect on transcription in the brain.

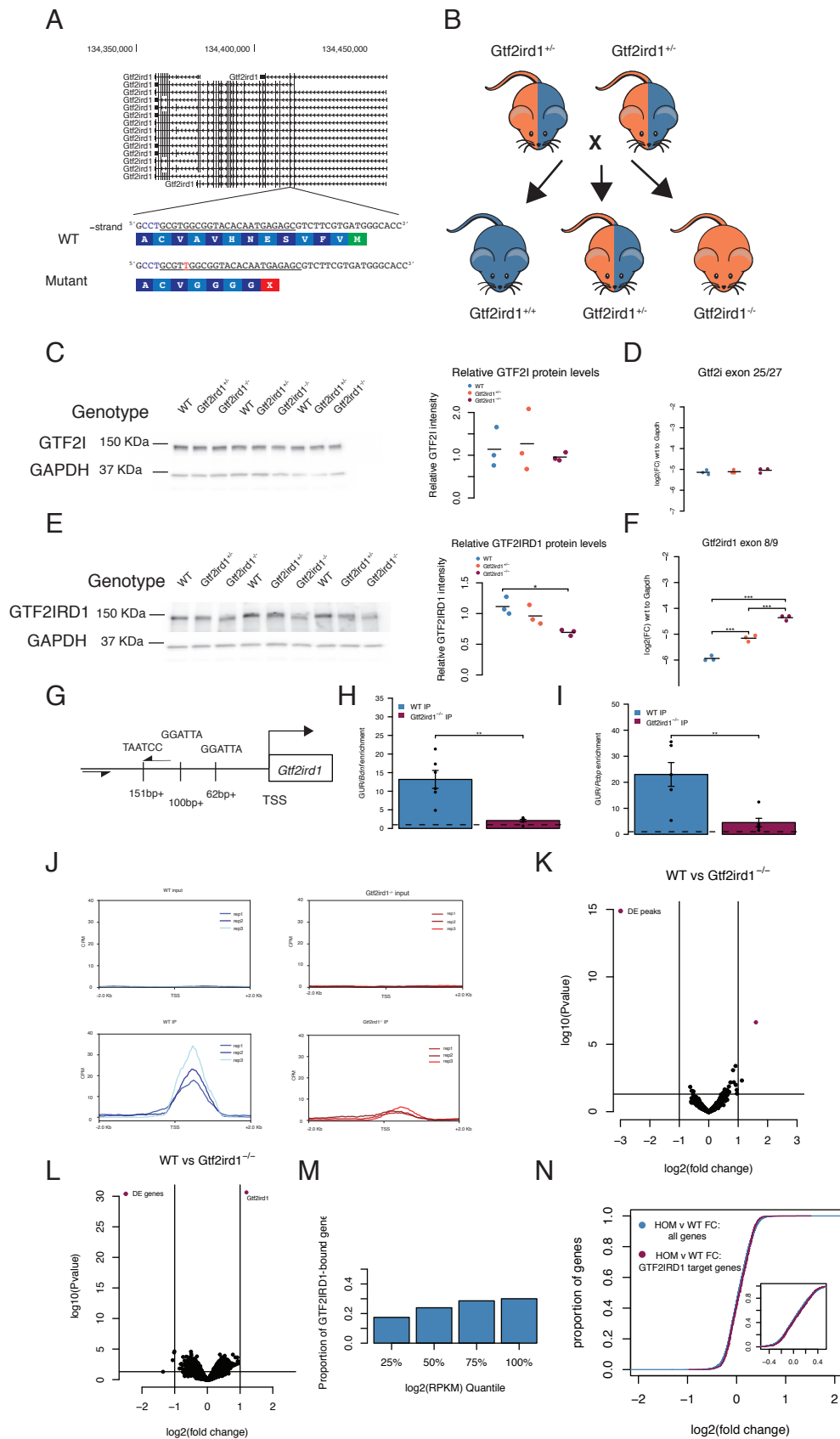


## Figure 5: Homozygous frameshift mutation in *Gtf2ird1* is sufficient to cause behavioral phenotypes.

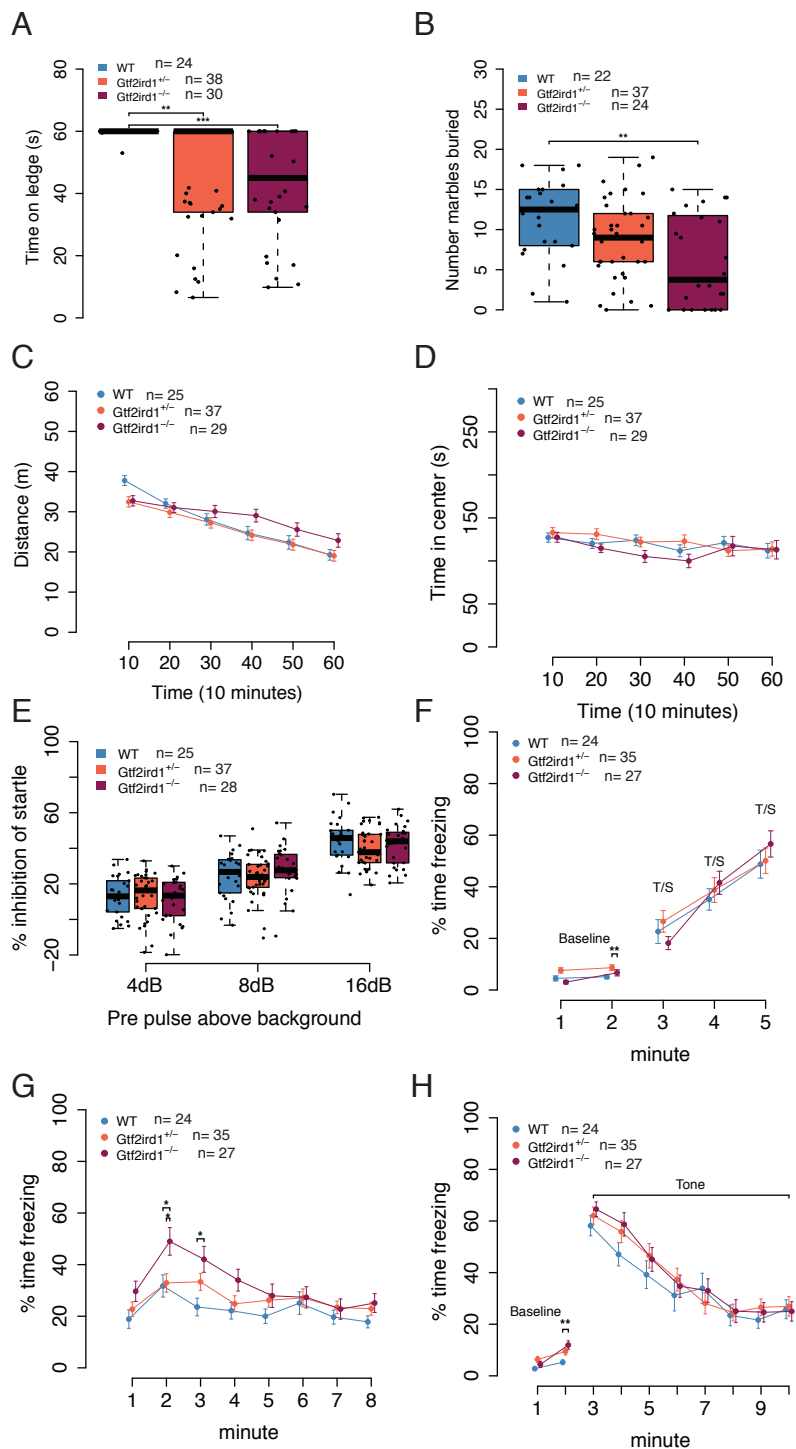


## Figure 6: Mutating both Gtf2i and Gtf2ird1 does not result in larger differences in brain transcriptomes.

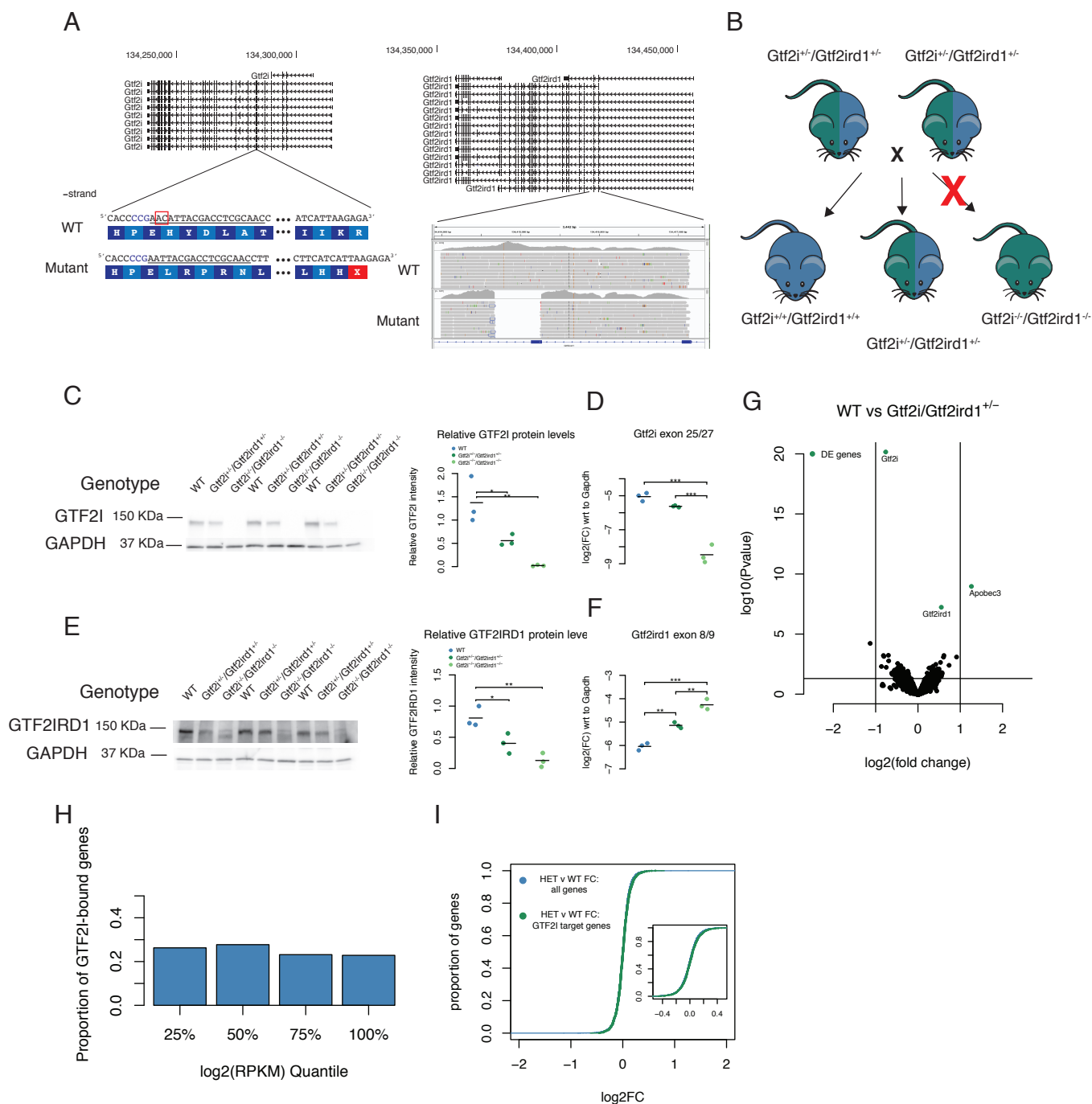


**Figure 7: Gtf2i does not modify most of the phenotypes of Gtf2ird1 mutation.**

